Matthias Heinisch, BSc

MultiFi:
Multi Fidelity Interaction with Displays On and Around the Body

MASTER'S THESIS

to achieve the university degree of

Master of Science

Master's degree programme: Computer Science

submitted to

Graz University of Technology

Supervisor

Dr. techn. Jens Grubert
Univ.-Prof. DI Dr. techn. Dieter Schmalstieg

Institute of Computer Graphics and Vision

Graz, June 2015

Deutsche Fassung:
Beschluss der Curricula-Kommission für Bachelor-, Master- und Diplomstudien vom 10.11.2008
Genehmigung des Senates am 1.12.2008

EIDESSTATTLICHE ERKLÄRUNG

Ich erkläre an Eides statt, dass ich die vorliegende Arbeit selbstständig verfasst, andere als die angegebenen Quellen/Hilfsmittel nicht benutzt, und die den benutzten Quellen wörtlich und inhaltlich entnommenen Stellen als solche kenntlich gemacht habe.

Graz, am …… ……..
(Unterschrift)

Englische Fassung:

STATUTORY DECLARATION

I declare that I have authored this thesis independently, that I have not used other than the declared sources / resources, and that I have explicitly marked all material which has been quoted either literally or by content from the used sources.

…… ……..
date (signature)

Abstract

Smartphones are commonly used to access information on the go, but their access cost can make them cumbersome to use in mobile scenarios. In particular, for micro-interactions, access cost may outweigh the time of actual interaction. Smartwatches and head-mounted displays are designed to eliminate access cost, but, on their own, they cannot match the usability of smartphones due to tiny screens and indirect input methods.

This work introduces MultiFi, a proposal to combine these three device types in a novel way by taking advantage of dynamic alignment of devices and widgets. It explores how the interaction seams occurring when interacting with devices of different fidelities can be overcome, putting the focus on interaction on-the-go. A prototype has been implemented in a laboratory environment in order to explore this design space, proposing a set of interaction techniques for such a multi-fidelity system.

A comparative user study was conducted that indicates that MultiFi can outperform alternative wearable device configurations for information browsing and selection tasks, albeit at the cost of lower usability ratings. In the process, verbal feedback has been collected that may prove useful for future research.

Acknowledgements

I would like to thank the following people that played a part in the completion of this thesis.

Jens Grubert provided me not only with his expertise on the relevant subjects, but also with a well organized project schedule and a large share of his time.

The opportunity to collaborate with him, Aaron Quigley and Dieter Schmalstieg on the scientific paper published in the course of this work is one I would not like to have missed.

Raphaël Grasset introduced me to the osgART toolkit, used in early stages of prototyping, and the Vuzix HMD.

Andreas Wurm was always helpful when I required tools or resources to build and set up the prototypical hardware system.

I greatly benefited from Dominik Hütter's work, which involved porting the DLT and SVD algorithms from C++ and Octave code to JavaScript.

This work uses a LaTeX template originally created by Pierre Elbischger.

Finally, I would like to thank my parents, extended family, friends, colleagues and my partner for their ongoing support throughout the years.

Contents

List of Figures

1 Introduction

This work introduces *MultiFi*, a proposal to combine handheld and wearable devices into a novel mobile user interface. This introductory chapter first explains the motivation behind this project, then highlights the contributions and limitations of this work and finally gives an overview of this work's structure.

1.1 Motivation

Within the last decade, an immense growth in the mobile computing market, thanks to the introduction of smartphones and tablets, could be observed. The so-called "phablets" are becoming a viable replacement for laptops and even desktop machines, due to the large progress in mobile computing power and the easy-to-pick-up touch based interfaces of these handheld devices.

Smartphones are the current state of the art for mobile usability with large high resolution displays, improving both the *output and input fidelity*. Yet, they are not *always-on* which impacts their *access cost*, especially on micro-interactions as a user needs to invest some time to pull a smartphone out of his or her pocket and put it away again.

The family of mobile devices is about to grow even further through the emergence of wearables: smartwatches are already gaining popularity on the mass market with products like Samsung's Galaxy Gear or Apple Watch. Google Glass and Epson's Moverio, among others, show that the technology is already here to provide the market with see-through head-mounted displays (HMD).

Wearable devices are always on and avoid access cost almost completely, which can give them an advantage over smartphones. However, these new devices come with their respective disadvantages: smartwatches and HMDs suffer from their comparatively *low fidelity*: smartwatches feature only small screens, impacting both input and output fidelity, while current affordable see-through HMDs suffer from limited input capabilities, low contrast and resolution.

Expecting an increase in popularity of these new wearable devices, this work started out as a desire to explore the design space that comes from combining these three device types into a novel kind of wearable user interface in which the simultaneous use of these devices can overcome the shortcomings of its individual parts by taking advantage of *dynamic alignment of devices and widgets*.

The result is *MultiFi*, a platform for designing and implementing user interface widgets across multiple displays with varying fidelities for input

and output. Typically, widgets such as toolbars or sliders are specific to a single display platform, while widgets that can be used between and across displays are largely unexplored. A possible reason for this may be varying fidelities of input and output across devices, making it difficult to apply a one-size-fits-all approach. Thus, development of MultiFi comes with various challenges to overcome and pitfalls to consider.

For input, different modes and degrees of freedom must be accommodated. For output, properties such as resolution and field of view may vary. If widgets are simply scaled in size to match the varying device fidelities, precision and exactness can be impacted significantly. Moving across devices can make the differences in fidelity apparent and introduce seams affecting the interaction. MultiFi aims to reduce such seams and combine the individual strengths of each display into a joint interactive system for mobile use.

1.2 Publication

A paper based on the work presented in this thesis has been submitted to and accepted at CHI 2015 [GHQS15]. The author of this thesis played a part in developing the concept of MultiFi (Chapter 3), implemented the prototype and examples discussed in this work (Chapters 3.3 and 4) and assisted in setting up and conducting the user study presented in Chapter 5. The paper can be seen as a condensed version of this work. As such, some text passages may be shared between the two works.

1.3 Contributions

This work addresses the design problem of interaction on the go across multiple mobile displays with the following contributions:

1. Exploration of the design space of multiple displays on and around the body and identification of key concepts for seamless interactions across devices.

2. Introduction of a set of cross-display interaction techniques.

3. Presentation of empirical evidence that combined interaction techniques can outperform individual devices such as smartwatches or head-mounted displays for browsing and selection tasks.

1.4 Limitations of the work

The subject introduced above is large enough to fill several master's theses and papers. Therefore the scope of this work is bounded by the following limitations:

1. This work explores only *single-user* interfaces. Allowing for multiple users to share information and combine their devices for an even larger interaction space may be the subject of future work.

2. There are many on-and-around-the-body devices that could be combined, or even completely new devices, that specialize, e.g., on spatial gesture input. The research in this work is restricted to using existing devices that are likely to become widely available to consumers in the coming years, based on observations of the current market development: smartphone, smartwatch and see-through HMD.

3. Focus of this work is put on researching mobile use *on the go*, with the user potentially walking. Thus this work knowingly avoids the use of (stationary) external screens and smart surfaces.

4. Creating a fully working outdoor prototype presents an engineering challenge of its own (tracking, networking and processing power, amongst other factors). Therefore, the laboratory-bound MultiFi prototype described in this work serves only as a proof of concept, while keeping in mind the restrictions that typically come into play in a mobile context. Future work will focus on bringing MultiFi into a truly mobile environment.

1.5 Structure

This introduction is followed by a chapter on related work, talking about *augmented reality* and *see-through calibration*, *wearable interaction*, *virtual display environments* and *multi-device interaction*, in preparation for the main part of this thesis.

Chapter 3 is dedicated to explaining the concept of MultiFi, a prototypical system developed in the course of this work, followed by details on its implementation in Chapter 4, in particular, the hardware that was used, the network structure and rendering.

A user study was conducted to compare multi-fidelity interfaces and traditional ones. The experimental design and results in regard to *error rate*,

task completion time and *user feedback*, both verbally and from questionnaires are presented in Chapter 5. Finally, the findings of the study and informal observations are discussed in Chapter 6.

To conclude, the final chapter 7 summarizes the work and gives an outlook on potential future work.

2 Related Work

In order to build a system as described in this work, a background on the subjects of augmented reality and see-through calibration is required. The first section of this chapter serves as an introduction to these topics.

Then related work in the fields of wearable interaction, virtual display environments and multi-device interactions is discussed, in order to give the reader an impression of today's state of the art, as well as to differentiate this work from existing efforts.

2.1 Augmented Reality

The term *augmented reality (AR)* describes the act of enhancing the real world with virtual elements. Typically, the term is used in the context of only visual augmentation [MTUK95], but in a broader definition, every sense such as smell, touch and taste may be augmented [MK94]. For this work, only visual augmentation is used.

Typically, AR systems require precise spatial registration (with six degrees of freedom) [A+97], with spatial registration methods available [WF02]. In MultiFi's case, up to two objects (a smartwatch and a smartphone) need to be tracked.

A common method of achieving augmented reality is to employ computer-vision based tracking methods [LF05]. In *video see-through*, virtual objects are superimposed on a live camera stream of the scene and then presented to the user, e.g., through a head-mounted display (like Oculus Rift) or smartphones. This method has the advantage of eliminating the perceived latency between the real world and the virtual content by simply delaying the video stream for synchronization [RHF95]. In turn, depth cues such as accommodation and defocus blur cannot be reproduced by current technology, and the latency is experienced on the real world, instead of the augmentation, potentially leading to virtual reality sickness.

MultiFi uses augmented reality to display virtual objects on an *optical see-through* head-mounted display. With this method, the real world is perceived naturally, but at the cost of the virtual scene potentially trailing behind and, thus, creating seams between real and virtual content. This has to be considered, when designing for optical see-through displays.

2.1.1 See-Through Calibration

MultiFi uses *see-through head-mounted displays* and relies on spatial relations between the devices. It is necessary to calibrate the system in such a way

that a virtual scene rendered on the display is aligned with the real world from the user's point of view. The underlying process is called *see-through calibration.*

The largest benefit of optical see-through displays is the absolute lack of latency in the user's perception of the real world, avoiding detachment of the user from the real world. Displays like the Google Glass or Epson Moverio are examples for this type of display. In turn, it is generally harder to create a seamless augmented reality experience, due to the latency between real world view and augmented content.

Calibration on video see-through displays is easier to automatically verify, as what the user sees is also "seen" by the system through the video stream that is displayed on the user's screen. For optical see-through displays, the target camera is the user's eye; this means that only the user can verify if the calibration was a success.

To achieve the see-through calibration in this work, Single Point Active Alignment Method (SPAAM) by Tuceryan et al. [TN00] was used. A projection matrix needs to be found that imitates the pinhole camera model set up by the eye as the camera position and the display as the projection plane of the real world. An equation that yields such a projection matrix requires corresponding pairs of 2D and 3D points. In such pairs, an object located at the given 3D position in the real world relative to the camera position is always seen at the corresponding 2D point on the projection plane.

In order to collect the corresponding pairs, the user consecutively aligns a set of 2D discs displayed on the HMD with a real point with a known world position. The world position of the HMD is tracked as well. The position of the target point relative to the HMD is the needed 3D world point, while the position of the 2D disc is the corresponding 2D image point.

As multiple 3D points can correspond to the same 2D point, the equation system set up does not feature a unique solution and needs to be approximated with a method such as direct linear transformation (DLT) [HZ04]. The resulting matrix can then be decomposed via singular value decomposition (SVD) into a projection and a view matrix respectively, suitable for OpenGL-like APIs.

Multi Point Active Alignment (MPAAM) is an alternative calibration method developed by Grubert et al. [GTMS10]. While users have to change their positions multiple times in order to get satisfying results, MPAAM uses multiple real world points at different distances while the user can remain in place. In turn, this method takes more effort to set up, in particular with the limitations of the tracking system used in this work, and SPAAM delivered sufficiently satisfying results.

For more details on the implementation in MultiFi, see Chapter 4.3.

2.2 Wearable Interaction

Today's dominant handheld devices, such as smartphones or tablets, have a high *access cost* in terms of the time and effort it takes to retrieve and store a device from where it typically resides, such as one's pocket. This cost reduces the usefulness of a device for micro-interactions, such as checking the time or one's message inbox.

Wearable devices such as a smartwatch or head-mounted display (HMD) lower the access cost to a wrist flick or eye movement. However, interaction with these *always-on* devices is encumbered by their low *fidelity*: Limited screen and touch area, low resolution and poor contrast compared to more powerful handheld devices limit what users can do. Currently, HMDs require indirect input through touch devices or envision high-precision spatial pointing, which is not yet commercially available on a satisfying level of quality. Despite these limitations, studies show that users expect the same or similar services on smartwatches as they are used to from smartphones [Joh14].

Recent research aims to improve the overall fidelity, investigating higher resolution and more immersive displays, improved pointing precision on touchscreen devices [OFH08, VB07] or physical pointing [CQG+11, DCN13]. Song et al. use standard cameras built into smart devices to track in-air gestures around the device [SSP+14]. Ahn et al. propose BandSense, a technology that recognizes touch inputs on the wrist band, thus, not obscuring the screen [AHY+15]. Audio is used for eyes-free wearable interaction in works of Brewster and Lumsden [BLB+03, LB03].

2.3 Virtual Display Environments

In order to extend display real-estate on wearable devices, several works employ virtual screen techniques [FMHS93, Fit93, Rei93].

Prominent design dimensions include the *spatial reference frame* and the *continuity of the display space* [WNG+13]. Popular frames of references are the physical screen itself, as in dynamic peephole metaphors using a fixed planar mapping [PHI+13], body parts on the user [CMT+12, LXC+14], the space immediately around the user [BS99, LDT09] or the world-referenced physical environment around the user [CB06].

The display space can be both continuous, as with virtual desktops, or discrete, e.g., when virtual display areas are bound to specific body parts [CMT+12]. Continuous display and input spaces can range from planar to curved surfaces [EFI14, PHI+13].

For instance, Ens et al. [EFI14] explored the design space for a body-centric virtual display space optimized for multi-tasking on HMDs and pin-

pointed relevant design parameters of concepts introduced earlier by Billinghurst et al. [BBDM98, BS99]. They found that body-centered reference frames can lead to higher selection errors compared to world-referenced layouts, due to unintentional perturbations caused by reaching motions. However, as MultiFi focuses on interaction on-the-go, world coordinates cannot be used as a general reference frame.

2.4 Multi-Device Interaction

Users with multiple devices tend to distribute tasks across different displays, because moving between displays is currently considered a task switch, while extending the input and output of several displays has received limited attention, in particular for mobile or wearable scenarios.

Yang and Widgor introduced a web-based framework for the construction of applications using distributed user interfaces, but do not consider wearable displays [YW14].

Research on interaction in mobile multi-display environments has focused both on fully aligned (i.e., spatially registered) cross-device interaction, including body parts as input and output devices [WNG+13] and on loosely coupled interaction across semantically associated, but spatially not tightly registered devices.

As an example of the latter, Duet combines smartphones with smartwatches and infers spatial relationships between the devices based on local orientation sensors [CGWF14]. Similarly, Billinghurst et al. [BGL05, BLB13] combine smartphone and HMD, but use the smartphone mainly as an indirect input device for the HMD.

To give examples for spatially registered interaction, stitching together multiple tablets allows for interaction across them, under the assumption that they lie on a common plane [HRG+04]. Several other approaches combine larger stationary with handheld displays through spatial interaction. Touch projector [BBB+10] allows for the transfer of content between displays using a smartphone and a raycasting metaphor. Benko et al. combine a touch table with an HMD [BIF05]. They use cross-dimensional gestures to transfer content between 2D and 3D displays.

While they used handheld displays in a stationary setting (as a magic lens for a tabletop system), this work focuses on the dynamic alignment of multiple body-worn displays, using body motion for spatial interaction. As large stationary displays restrict mobility, virtual screen environments seen through a HMD may be a suitable replacement in the mobile context of MultiFi.

3 The Concept of MultiFi

During the writing of this work a proof of concept for such a multi-fidelity, multi-device system was developed: *MultiFi*. This chapter introduces the concept, describing design factors, explaining design decisions and, finally, giving some examples, both in the form of prototypically implemented widgets as well as a possible scenario, in which the MultiFi system is used. This chapter provides the first two contributions listed in Chapter 1.3, with the design space explored and key concepts identified in Chapter 3.2 and interaction techniques presented in Chapter 3.3.

3.1 Devices

MultiFi employs three different types of devices: a *handheld smartphone or tablet (HHD)*, a *wearable smartwatch (SW)* and a *head-mounted display (HMD)*. At the time of writing, MultiFi uses only a smartphone, but no tablet. The reader may assume that the term handheld in the remainder of this work refers only to smartphones, unless otherwise specified.

Each of these device types comes with a set of advantages and disadvantages: The handheld, especially the smartphone, can be considered the state of the art for mobile interaction. It comes with a large input and output area, a high resolution display and allows two-handed interaction. The downside of handheld devices is their *access cost*, in particular in a mobile scenario, where smartphones are stored in the user's pocket, and tablets, even in bags.

Being wearable, the smartwatch and head-mounted display eliminate access cost almost entirely. In turn, these devices have a hard time matching a handheld device's usability: smartwatches feature only a very small touch screen, inherent to their purpose, which may cause frustration for prolonged interactions or when navigating a larger information space. In its worn state, a smartwatch can only be operated by one hand.

The head-mounted display by itself features no unified input area at all. Various manufacturers have attempted to solve this challenge in different ways. Examples include clunky external handheld touch pads, which take away the head-mounted display's wearable property and Google Glass's touch pad mounted on the user's temple. However, methods like these only enable indirect input. Another weakness of current consumer see-through HMDs is their inconsistent display quality. Different lighting conditions may negatively impact the contrast and visibility on such devices, potentially lowering the head-mounted display's output fidelity compared to the screens of handheld devices and smartwatches.

MultiFi aims to leverage the advantages of the wearable devices (smart-

watch and HMD) in order to overcome these weaknesses and allow them to keep up with the established handheld devices in both interaction fidelity and speed. Furthermore, micro-interactions may benefit from such a wearable multi-fidelity system, due to the potentially significant reduction in access cost.

Additionally, MultiFi explores how the handheld can be added to the combination for novel interaction techniques, particularly in rested positions where the user has the time to occupy both hands for prolonged interactions, e.g., on a bus, at home or on a park bench.

3.2 Interaction by dynamic alignment

Using these three different devices, their spatial relations constantly change. The handheld may be in the user's hands or tucked away in a pocket on the user's body. Both the smartwatch and handheld may be in view or out of view. Forcing the user to constantly hold the smartwatch or head-mounted display in a specific position relative to each other may cause fatigue and discomfort. Having the devices spatially completely independent from each other leaves out a big part of the potential interaction space. MultiFi operates somewhere in between and proposes *dynamic alignment of devices and widgets* to make use of the situationally dynamic spatial relations between devices and to leverage the complementary fidelities of the devices.

Dynamic alignment can be seen as an application of proxemics [GMB+11]: Computers can react to users and other devices based on factors such as distance, orientation, or movement. In MultiFi, dynamic alignment changes the interaction mode of devices based on a combination of proxemic dimensions. This work focuses on *distance* and *orientation* between devices. However, different alignment styles can be explored, which are location-aware, vary between personal and public displays or consider movement patterns.

3.2.1 Design factors

Development of user interfaces benefits from finding and understanding the underlying design implications. The following design factors have been determined before and throughout development of MultiFi.

Spatial reference frames encompass where in space information can be placed, if this information is fixed or movable (with respect to the user) and if the information is a tangible physical representation (i.e., if the virtual screen space coincides with a physical screen space) [EHRI14].

Direct vs. indirect input In the context of this work, the term direct input is used, if input and output space are spatially registered, and indirect input, if they are separated. As a consequence of allowing various spatial reference frames, both direct and indirect input must be supported. Smartphones are a good example for direct input: The user can *directly* interact by touching what is seen on the screen. An example for indirect input is a touch pad like that of Google Glass or the trackpad of a laptop.

Fidelity concerns the quality of individual devices' output and input channels such as spatial resolution, color contrast of displays, focus distance, or achievable input precision. Screen size also contributes to fidelity, as larger screens can show more (detailed) information, while smaller screens are more cumbersome to interact with. Higher fidelity may be required if more information needs to be displayed. Distributing information appropriately to accommodate for the different devices' fidelities is a key challenge in MultiFi.

Continuity When combining multiple devices in one way or another, a challenge is found in dealing with continuity seams in both output and input. Continuity can be negatively impacted by differing device fidelities, in particular, if a single piece of information lies across the border between two devices. Another factor to be considered comes from continuity gaps caused by, e.g., bad registration or bezels. Information split across two devices may lead to transition issues, e.g., on two devices with different focus planes, a user may need some amount of time to accommodate upon a focus switch.

If the output of one device (e.g., SW) is extended using a second device (e.g., HMD), input may not be extended. This can lead to usability issues, such as users associating the extension of the output space with extension of the input space.

Since many of these continuity seams can not be fully avoided with multi device setups, a significant portion of the design work for a system like MultiFi is to figure out how to deal with these seams and mitigate their negative impact on the overall experience.

Social acceptability Wearable interaction may benefit from movements of the body, in particular, the head and the arms. However, not all situations may be suited for heavy use of large gestures, and observers may deem it socially unacceptable to physically interact in a virtual environment only visible to the user, in particular, in crowded places, where there may not be sufficient room for anything but small gestures. Studies of interactions

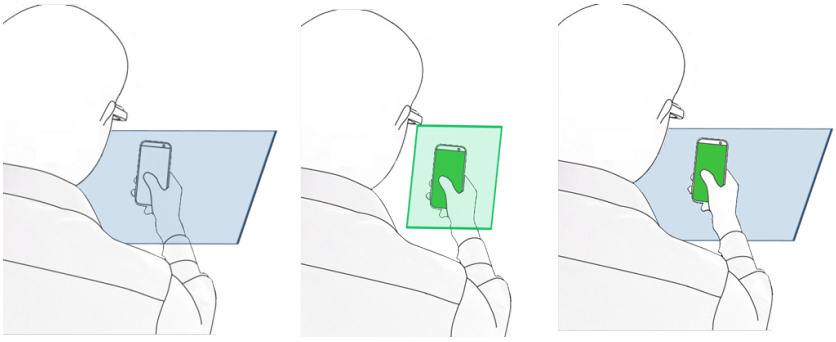

Figure 1: Body-aligned mode (left), device-aligned mode (middle) and side-by-side mode (right)

with mobile, on and around body devices [RB09] reveal the personal and subjective nature of what is deemed acceptable.

Dynamic alignment offers the opportunity to give users a choice in their preferred alignment mode, depending on context factors including the technology, social situation or location.

3.2.2 Alignment modes

For the combination of HMD and touch device, three possible alignment modes are distinguished in this work (see Figure 1).

Body-aligned mode In this mode, the devices share a common information space, which is spatially registered to the user's body. The head-mounted display allows to get a low-fidelity overview of the body-referenced information space, while the touch screen of the touch device provides a high-fidelity inset for direct interaction. Unlike common spatial pointing methods the touch screen provides a haptic input space, making the slice of the information space displayed on the touch device more intuitive to interact with.

While wearable information displays could be placed anywhere in the 3D space around the body, this work focuses on widgets in planar spaces, as suggested by Ens et al. [EHRI14].

Device-aligned mode Here the information space is spatially registered to the touch device and moves with it. The HMD *extends the screen space* by displaying additional peripheral information at lower fidelity, comparable to focus+context displays [BGS01]. This information can be displayed continuously, mimicking a virtual large screen with a limited input window, or arranged in discrete units around the touch device.

Side-by-side mode Finally, in this most loosely coupled mode interaction is merely redirected from one device to another with no spatial relationship between devices required. A simple example is to use the smart watch as a touch pad to indirectly control a cursor on a body- or head-referenced information space displayed only on the HMD. The touch device may display related information or input interfaces such as the surroundings of the cursor on the HMD or a toolbox. When the touch device is outside of the user's field of view, its touch screen can still be used blindly.

3.2.3 Navigation

The principal input capabilities available to the user are spatial pointing with the touch device or using the touch screen.

Body-aligned mode lends itself well to spatial pointing. When the user's point of view, the device and the virtual plane in the information space are aligned along a ray, the HMD clears out the area covered by the touch device, and a high resolution inset is displayed on the touch device. Selected items can be moved in the information space by employing gestures such as holding a finger on the touch screen. This form of drag and drop can be very fast, but extended use is likely to lead to fatigue.

In device-aligned mode, spatial pointing fulfils more of a passive role, as moving the device moves the entire information space with it. While this combination does no longer allow selection, it supplies an overview of the information space. Active navigation can be achieved by classic touch screen gestures such as swiping or pinching. Using a small display like that on a smartwatch, this method can be inefficient for larger distances, but it seems just right for minute interaction.

Finally, in side-by-side mode, indirect navigation via touch gestures on the touch device occurs naturally, in particular, when the touch device is out of view, operated blindly. This kind of lean-back experience may induce the least physical fatigue, but it may be frustrating to make fine grained selections through the indirect interface.

Due to these very different and situation dependent advantages and disadvantages, no mode can be singled out as the absolute best. Therefore, the concept of dynamic alignment in MultiFi allows to switch modes on the fly. A user could first narrow down the search area using body-aligned mode, and then, switch to device-aligned mode to execute a precise selection, e.g., on a map. The switch could be performed with intuitive input metaphors, such as holding the map onto the smartwatch with one's finger or pressing a "hook switch".

In another scenario, a user could casually navigate the information space

with very low requirements of accuracy using the indirect side-by-side mode, then bring the touch device into the view, triggering body-aligned mode, to make a precise selection, e.g., scrolling down on a website using swiping gestures to read it and, then, precisely tapping one of several links, after the smartwatch has been brought into alignment.

3.2.4 Focus representation and manipulation

When working with multi-fidelity devices, there are several ways how higher fidelity can be used to set a focused element apart from its lower fidelity counterpart.

Visual Level of Detail The first and simplest option is to solely take advantage of text and icons being inherently easier to read on the higher fidelity device. Aligning the touch device with a piece of information on the information plane would work akin to a magnifying glass. An example can be seen in Figure 4.

Semantic Level of Detail [PF93] Alternatively, normally invisible information could become visible through such an alignment, using a *magic lens metaphor* [BSP+93]. For example, on the HMD, elements may be represented by simple icons, and aligning the touch device makes labels appear on it. Figure 3 shows an example in which aligning a smartphone with a tile on the HMD makes an interactive version of that tile appear on the handheld. Similarly, in Figure 5 (bottom row), the handheld shows a richer variation of a widget group including photos and detailed text, once it is aligned with the low fidelity representation on the user's arm.

Cascaded Interaction An interactive focus representation on the touch device can naturally be operated with standard touch widgets. In body-aligned mode, this leads to a continuous coarse-to-fine *cascaded interaction*: The user spatially points to an item with a low fidelity representation and selects it with dwelling or a button press. A high fidelity representation of the item appears on the touch screen and can be manipulated by the user through direct touch (Figures 3, 5).

For simple operations, this can be done directly in body-aligned mode. For example, widgets such as checkbox groups may be larger than the screen of a SW, but individual checkboxes can be conveniently targeted by spatial pointing and flipped with a tap.

Rubber Band Holding the touch device still at arm's length or at awkward angles may be demanding for more complex operations. In this case, it may be more suitable to *tear off* the focus representation from the body-aligned information space by automatically switching to side-by-side mode. A rubber band effect snaps the widget back into alignment, once the user is done interacting with it. This approach overcomes limitations of previous work, which required users to either focus on the physical object or on a separate display for selection [DCN13].

3.3 Example Widgets

MultiFi aims to simplify the design process for multi-fidelity applications. With the prototype developed in the course of this work, the following examples for cross-display interaction techniques have been created.

3.3.1 Lists

Smartwatches offer limited screen space, thus navigating a long list can become tedious for a user very quickly. With MultiFi, the view space is enlarged by augmenting further list items via the HMD to give the user a better overview, while keeping the size of the wearable device small, as seen in Figure 2. In order to minimize disparity between the devices caused by registration errors, the list is scrolled discretely (always snapping to the closest list item). In this way, list items will never be displayed across device boundaries. Optionally, a preview of the currently focused item can be displayed on the side of the smartwatch.

3.3.2 Menus

Menus with many togglable switches and selections may be tedious to browse on a small screen, as the view has to switch between an overview and detailed view. MultiFi allows to show the the overview on the HMD and the detailed view on the smartwatch or smartphone at the same time. A user can switch between the detailed views intuitively by aligning their device with the non-interactive tile representation of the desired option set on the HMD (see Figure 3). Changes on the smartphone are synchronized on the HMD in real time. In the example given, this are just textual updates, but the same approach can be used for more intricate scenarios, such as toggling filters for a map, while the map can be seen changing in the background.

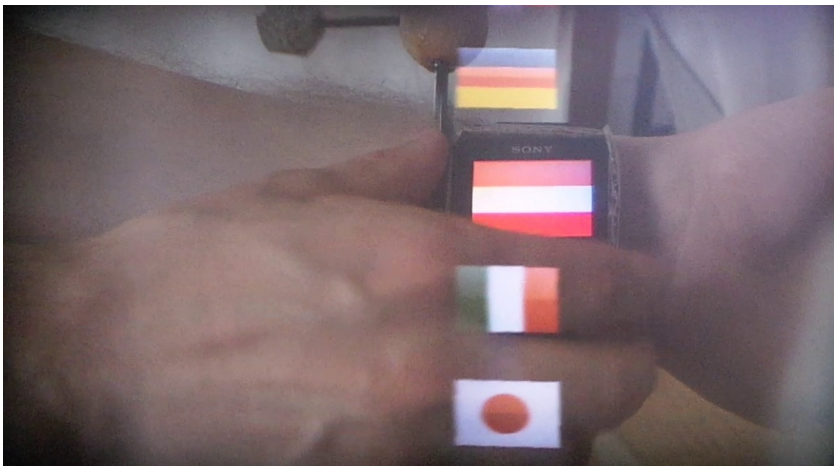

Figure 2: A discretely scrolling list taking advantage of the extended screen space to increase the overview

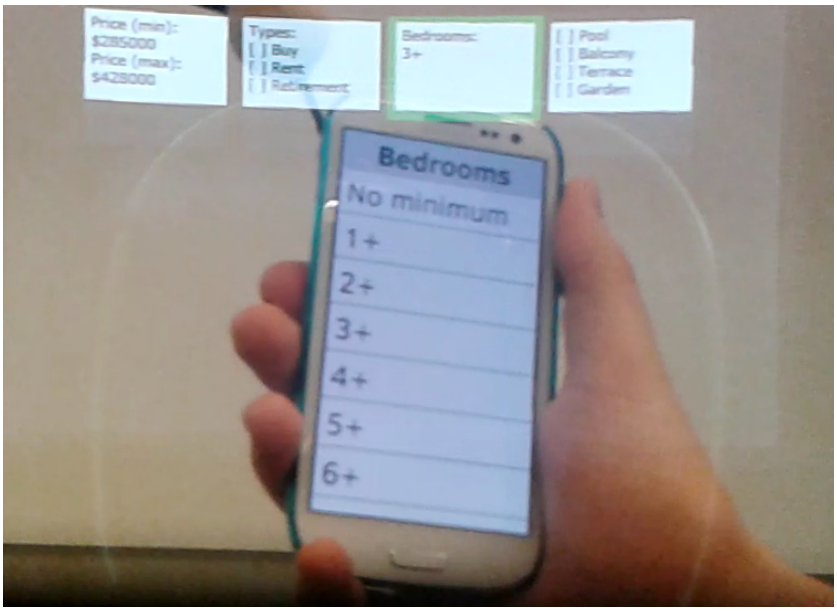

Figure 3: The option tiles on the HMD yield interactive versions of themselves on the smartphone, when it is aligned with them

Figure 4: The extended screen space metaphor for showing a map across smartphone and HMD

3.3.3 Map

A map widget has been implemented in multiple ways. The first version is called *smartwatch referenced* and essentially extends the concept of the ring menu to the second dimension and continuous navigation (which is desirable on a map). The map is displayed in a *focus+context* [BGS01] manner on the devices, with the smartwatch showing a high-fidelity and interactive portion of the map, while the HMD augments the context around it. The rectangle corresponding to the smartwatch's position on the HMD is not rendered in order to not interfere with the smartwatch's screen.

The second version, *body referenced*, displays the map in front of the user with respect to her body, similar to a vendor's tray, and the smartwatch can be moved over the map in a way similar to a magnifying glass. The area covered by the smartwatch on the HMD is displayed on the smartwatch in high fidelity and can be interacted with.

A third version combines these two approaches and lets the user switch between smartwatch referenced and body referenced with a simple input command such as holding or not holding the finger on the smartwatch, double tapping or pressing an (on screen) button.

3.3.4 Arm Clipboard

The arm clipboard uses the HMD to augment widgets relative to the user's lower arm. If a user wants to keep information ready for a quick glance, but does not want to clutter the view, this is an interesting proposition, as the arm can be moved in and out of the view at will to display or hide the information displayed on it.

A user can interact with the widgets on the arm by aligning the smartphone with the widgets, or, alternatively, by cycling through them using the smartwatch. The smartwatch would then offer a minimal interactive version of these widgets, while the smartphone may provide a higher fidelity version which can be "torn off" the arm and manipulated comfortably with both hands.

While the implementation presented here uses only the arm, the concept can be extended to any body referenced information storage. Existing body-centric widgets for handheld devices [CMT+12, LDT09] rely on proprioceptive or kinesthetic memorization due to the small field of view on handhelds, while this method makes use of the additional HMD to give the user an overview without having to use their smart devices to "scan" the body.

3.3.5 Text Input

Soft keyboards on smartphones typically suffer from too small buttons, and even then, many keys that are featured on desktop keyboards are still missing and require a mode switch or long presses of buttons to use them. At the same time, the screen space reserved for displaying the user-typed text is so small - often only one or two lines - that it is usually required to switch off the soft keyboard to get sufficient overview.

MultiFi approaches this challenge by making the smartphone's whole screen available as a soft keyboard, which allows to place all of a desktop keyboard's buttons in a comfortable size on it. The text output is relegated to a virtual screen on the HMD, which, from the user's point of view, protrudes from the top of the smartphone reminiscent of a clamshell design or extensible keyboard.

Further development of this system could include a simple swiping gesture to pull the text area down onto the smartphone to directly interact with it, e.g., to highlight text or position the caret. Alternatively, the text box could be fixed on the HMD, and the mode switch would be triggered by an intuitive alignment of the smartphone with the text box.

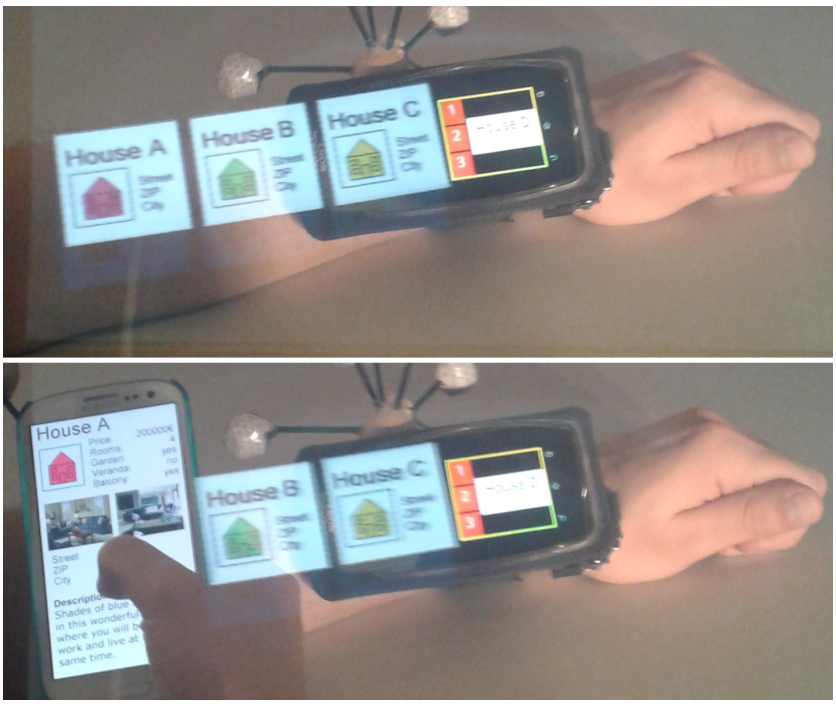

Figure 5: Arm clipboard with preview icons laid out on arm (top). Spatial pointing enables switching to high fidelity on a smartphone (bottom).

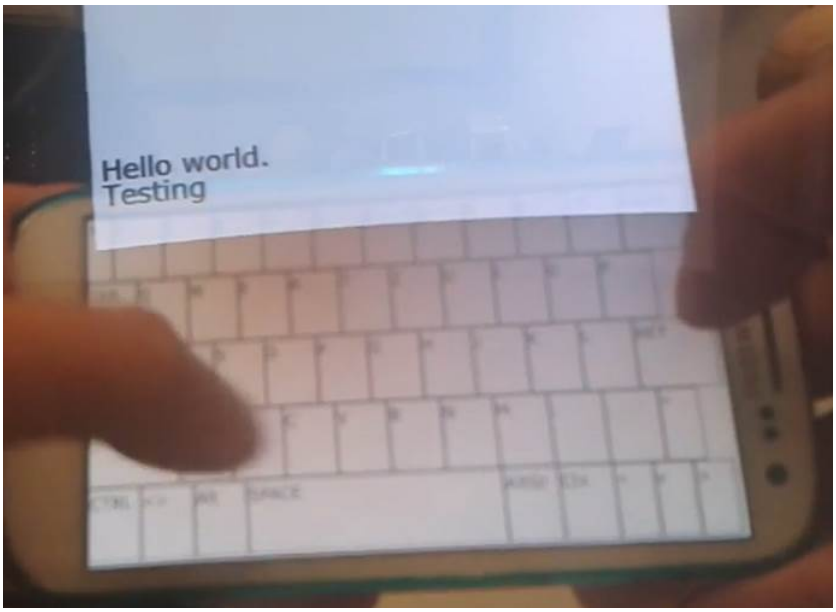

Figure 6: Full screen soft keyboard on a smartphone, while the text is displayed above using the HMD

3.4 Usage Scenario

This section demonstrates how MultiFi can aid in a house hunting scenario. The user Alice is looking to buy a new house. The widgets she uses in this scenario have been prototypically implemented, and described in Section 3.3.

First, Alice prepares at home by browsing a map of potential new homes using her HMD (Figure 7, a). She had previously narrowed down her search by using a filter application: She gets an overview of various parameters displayed on her HMD, grouped in tiles (Figure 3). Aligning her smartphone with a tile in her view, the smartphone displays an interactive and higher fidelity version of this tile, aided by the larger screen space and higher resolution offered by the smartphone compared to the tile displayed on the HMD. While adjusting a particular setting, she can still see the other tiles for context and with a flick of her wrist switch to another tile. On another view displayed in her HMD, she would see the points of interest on the map change in real time.

Happy with her choice, Alice leaves the house, and, while walking, she wants to select some waypoints from the map on the go. The HMD displays a body-referenced map in front of her, similar to a vendor's tray. By aligning her smartwatch with this map, she can interact with the patch of the map that is covered by the smartwatch (Figure 10).

Alice can browse house data sheets directly through a list on her smartwatch (Figure 7, b). This list takes advantage of extended screen space and shows elements of the list outside of the smartwatch's view on the HMD, but aligned with the smartwatch. Next to the smartwatch, she also sees a more detailed view of the currently selected item. Alice can select houses of her choice and arrange them on her arm, for example by a swiping gesture or the press of an on-screen button.

At a later point of the day, she wants to compare these houses on her arm. Essential details can be compared all at once by just looking at her arm through the HMD. Aligning her smartphone with one of the data sheets makes a higher fidelity version of it appear on the smartphone (Figure 5).

Having decided that she wants to take a guided tour of a particular house, Alice uses a full screen keyboard on her smartphone to email her real estate agent (Figure 6). Later on the go, she receives a notification from him, with a longer email giving his initial thoughts on the house along with some pictures. Alice can view the email on her HMD and casually swipe on her smartwatch, as if it was a touchpad, to scroll up and down (Figure 7, c).

Satisfied with her day of house hunting, Alice returns home.

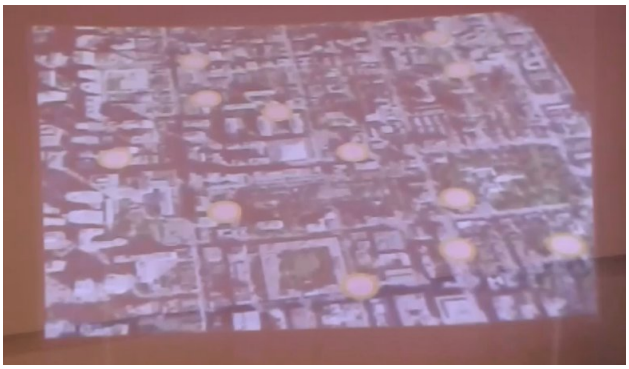

(a)

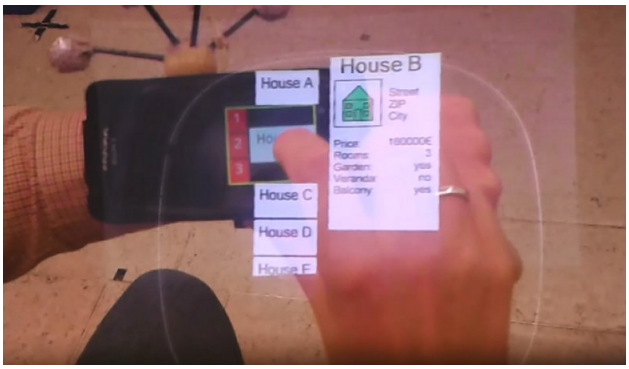

(b)

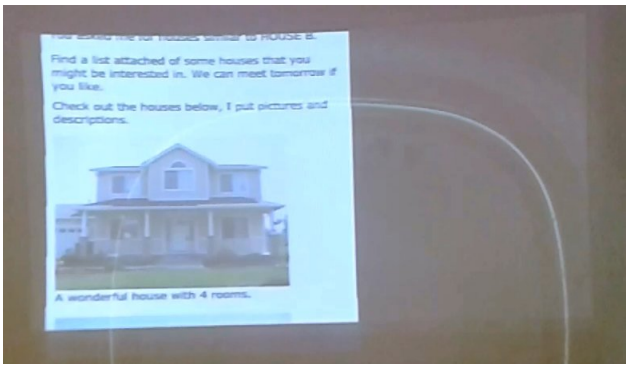

(c)

Figure 7: a) viewing a map on the HMD in body-aligned mode, b) list with preview in device-aligned mode, c) reading an email in side-by-side mode

4 Implementation

As a novel concept was explored with MultiFi, a cross-platform solution was needed that is easy to experiment with and enables rapid prototyping.

This prototype was implemented using two smartphones (*Samsung Galaxy SIII, Sony Xperia Z1 compact*) and a see-through HMD (*Vuzix STAR 1200XL*). The *Sony Xperia Z1 compact* was mounted to the forearm using a sport sleeve for the user's arm. This approach was chosen to simulate next generation smartwatches with higher display resolution and more processing power. To this end, the screen extent was limited to 40x35mm to emulate the screen size of a typical smartwatch.

Using a smartphone as a smartwatch further simplified prototyping, because it allowed to use a web browser on all devices and avoided the need of device-specific programming, offering a convenient match for the above mentioned requirements. Modern smartphones run browsers with a sufficient feature set to take advantage of WebGL for 3D rendering as well as WebSockets for networking. Additionally, the JavaScript language is a simple tool for quick scripting and is bound by no dependencies, besides the requirement for a relatively modern browser. Therefore, everyone who would like to use the tools developed during this work for more prototyping would not need to adapt the code, apart from some configuration, such as the size of the devices and the network environment. Another convenient advantage of a web browser based solution is that HTML can be used to quickly model classic user interfaces.

The following subsections will talk about network structure, rendering and calibration used in the prototype in more detail.

4.1 Infrastructure

A central Java-based application server manages all communication. The network structure can be seen in Figure 8. All client devices open a website in a browser and connect to the application server through WebSocket. Status updates originating from one client are distributed via the central server to the other clients. The server also receives tracking data, and forwards it to the smart devices. Messages are encoded in JSON for transmission. The used WebSocket solution for Java was taken from `http://java-websocket.org/`.

The Advanced Realtime Tracking (ART) outside-in tracking system was used to determine the 3D positions and orientations of all devices and sends them to the application server via VRPN (Virtual-Reality Peripheral Network) [TIHS+01]. For practical use, an inside-out tracking system would be preferable.

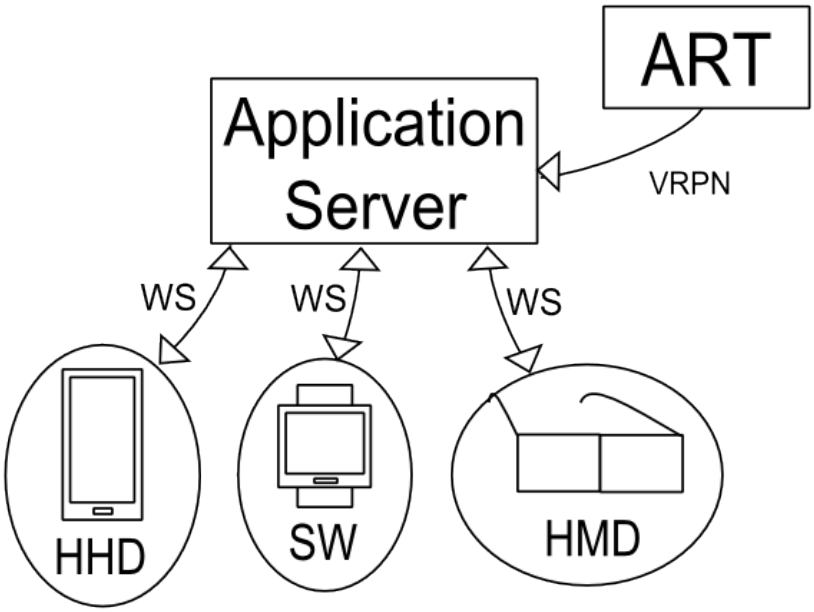

Figure 8: Diagram showing the network architecture

4.2 Rendering

3D and 2D graphics are rendered using the WebGL-based *THREE.js* scene graph library [Cab10]. For easier development, a framework has been written that wraps the most essential camera handling into JS objects in such a way that three camera types can be used interchangeably: stereo (two cameras side by side), mono (one camera) and orthographic (one camera without perspective). For MultiFi, only the stereo and orthographic mode are used for the HMD and touch devices respectively.

This allows to share a single scene graph representing the application status between the devices and look at it from different camera angles. Each device receives its own copy of this shared scene graph, which is synchronized across devices using the WebSocket updates. In order to avoid synchronization conflicts, one device, typically the smartphone or smartwatch, acts as the *primary* with the other device(s) acting as *replicas*, or each device is responsible for a certain part of the scene graph.

Furthermore, plain HTML (with JavaScript) was used to model generic user interfaces on the smartphone or smartwatch, where appropriate, e.g., for the full-screen keyboard or the filter widget.

4.3 Calibration and Registration

As virtual elements displayed on the HMD need to be aligned with real world objects (in this prototype, only the smartwatch and the smartphone), the HMD needs to be calibrated accordingly. Additionally, screen positions need to be registered to their tracking markers.

For calibration, SPAAM (Single Point Active Alignment Method) [TN00] was implemented (see also Section 2.1.1). The corresponding points are determined by aligning a virtual point displayed on the HMD with a real marker with tracked position by moving the head and tapping the smartphone screen to confirm the perceived alignment and advance the next point.

Stereo calibration is achieved by showing the same point set first to the left and then to the right eye, with the other eye, respectively, only seeing a blank screen. This approach was chosen, because direct stereo calibration suggested by Genc et al. [GSW+00] would add complexity to the process of alignment or require additional input to adjust the disparity between the displays.

The implementation of the direct linear transformation and singular value decomposition is based on the method shown by Hartley and Zisserman [HZ04] and was implemented in JavaScript using *numeric.js*. The resulting projection and view matrices for each eye are saved in a configuration file stored in a folder named after the user's profile.

Registration of device screens (smartwatch and smartphone) to their markers happened by aligning a virtual rectangle of the same size with the real screen, viewed through the already calibrated HMD. Through a tap of the screen, the virtual screen switches its fixture from the HMD to the device, and back with a second tap. In this way, fine tuned alignment is possible. This process is illustrated in Figure 9.

Verification of the registration was purely visual, requiring the user to move and turn the device and observe discrepancies between the virtual plane and the real screen. This process is rather unstable and requires a lot of patience on the part of the user, but since users participating in the user study did not have to perform this registration by themselves, this simple approach was sufficient for the purpose of this work.

Using a camera equipped computer to perform the alignment should provide much more accurate results. This is possible because, unlike see-through calibration, device screen registration is not dependent on the viewer. Should trackable smart devices be produced industrially in the future, manual registration may not be necessary at all, as the relative positions of tracking marker and screen are already known from the design process.

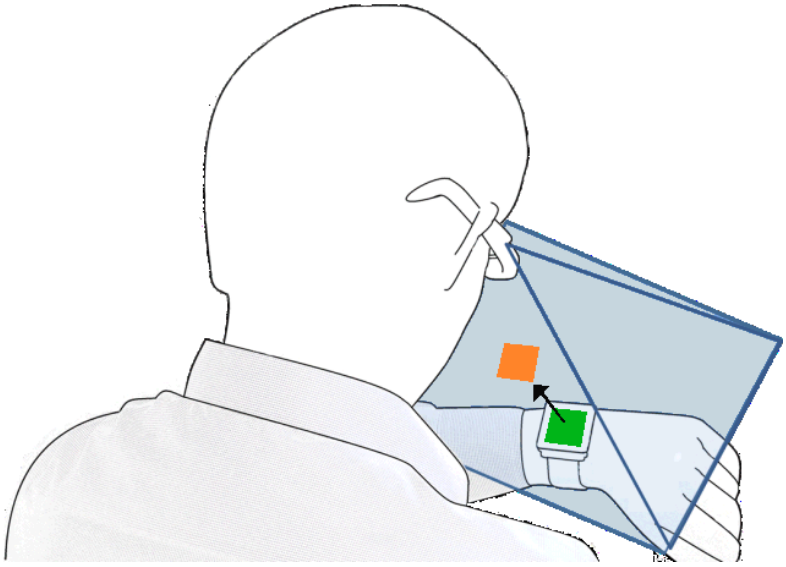

Figure 9: Registration of smartwatch screen to smartwatch tracking marker. The user aligns the device screen (green) as precisely as possible with the equally sized virtual rectangle seen through the HMD (orange). A tap on the smartwatch's screen fixes the position of the orange rectangle relative to the smartwatch for visual confirmation. Tapping again fixes the rectangle back to the HMD, allowing for fine tuning.

5 User Study

A laboratory user study was conducted to investigate if combined device interaction can be a viable alternative to established single device interaction for mobile tasks. The focus for the user study was put on two tasks: information search and selection. These tasks were chosen so they can be executed on the go and underpin a variety of complex tasks. This study serves as the third contribution listed in Chapter 1.3, providing empirical evidence that combined interaction techniques can outperform individual devices, such as smartwatches or head-mounted displays, for browsing and selection tasks.

5.1 Experimental Design

A within-subjects study was designed to compare the performance and user experience aspects of MultiFi interaction to single device interaction for two information browsing tasks. The independent variable for both tasks was an interface with five levels:

1. *Handheld (HHD)* - The Samsung Galaxy SIII was used as only input and output device. This serves as the baseline condition for a handheld device with high input and output fidelity.

2. *Smartwatch (SW)* - The wrist-worn Sony Xperia Z1 compact was used as only an input and output device. The input and output area was 40x35 mm and highlighted by a yellow border, as shown in Figure 10. Participants were notified by vibration if they touched outside the input area. This condition serves as baseline for a wearable device with low input and output fidelity (high resolution, but small display space).

3. *Head Mounted Display (HMD)* - The Vuzix STAR 1200XL was used as an output device. Indirect input was employed as in the SW condition, using a control-display ratio of 1, with the touch area limited to the central screen area of the HMD. This condition serves as the baseline for a HMD with low input and output fidelity, which can be operated with an arm-mounted controller (without the need for retrieving the controller from a pocket).

4. *Body-referenced interaction (BodyRef)* - The content was displayed in front of the participant's upper body above a table (Figure 1, left). The HMD was used to control the user's viewpoint of the virtual scene. The touch screen of the smartwatch could be used to control the position and scale of the virtual map in front of the body using the same input

options as in SW, HMD, SWRef (see below). In addition, selection was achieved by aligning the smartwatch, with the target visible in front of the user and touching the target rendered on the smartwatch.

5. *Smartwatch referenced (SWRef)* - The information space was displayed relative to the smartwatch screen (Figure 1, middle). Outside the smartwatch screen, the virtual content was visible in the HMD, employing the extended screen space metaphor. As in BodyRef, the HMD was used to control the user's viewpoint of the virtual scene. The information space could be panned and zoomed as in the other conditions.

In both tasks, dependent variables of interest were *task completion time, errors, subjective workload* as measured by NASA TLX [HS88] as well as user experience measures (After Scenario Questionnaire (ASQ) [Lew91], *hedonic and usability aspects* as measured by AttrakDiff [HBK03]) and overall *preference* (ranking).

5.2 Apparatus and Data Collection

The study was conducted in a controlled laboratory environment. A Samsung Galaxy SIII (resolution: 1280x720 px, 306 ppi, screen size: 107x61 mm) was employed as a smartphone, a Vuzix STAR 1200 XL HMD (resolution: 852x480 px, horizontal field of view (FoV): 30.5° vertical FoV: 17.15°, focus plane distance: 3 m, resolution: 13 ppi at 3 m, weight with tracking markers: 120 g) and another smartphone (Sony Xperia Z1 compact) as a smartwatch substitute (resolution: 1280x720 px, cropped extent: 550x480 px, 342 ppi, weight with tracking markers: 200 g). The HMD viewing parameters were matched with virtual cameras which rendered the test scenes used in HHD, HMD and SW. Thus, all conditions operated in coordinate systems with the same metric units. The translation of virtual cameras for panning via touch in all conditions parallel to the screen was set to ensure a control-display ratio of 1. Pinch to zoom was implemented by the formula $s = s_0 \cdot s_g$, with s being the new scale factor, s_0 the map's scale factor at gesture begin and s_g the relation between the finger distances at gesture begin and end.

While the system is intended for mobile use, here participants conducted the tasks while seated, due to the strenuous nature of the repetitive tasks in the study. The participants were seated on a table (120x90 cm, height 73 cm). The chair was height adjusted for individual participants to ensure that its armrests are at the same height as the table. This should mitigate expected fatigue effects, which could arise during the repetitive nature of the tasks.

Data was collected for evaluation through automatic logging on the test devices, questionnaires, video recording and semi-structured interviews at the end of the study. For data analysis, R and SPSS were used. Null hypothesis significance tests were carried out at a .05 significance level, and no data was excluded, if not otherwise noted. For ANOVA, Mauchly's test was conducted. If the sphericity assumption had been violated, degrees of freedom were corrected using Greenhouse-Geisser estimates of sphericity. For the sake of readability, only the most relevant findings are reported within the main text. The complete test statistics are attached in the appendix (Sections A.2 and A.3). For all figures, brackets indicate significant difference with a p-value <0.05 (*) and <0.01 (**). Error bars indicate standard deviation.

5.3 Procedure

After an introduction, signing an informed consent form and completing a demographic questionnaire, participants were introduced to the first task (counterbalanced) and the first condition (randomized). For each condition, a training block was conducted. For each task, participants completed a number of trials (as described in the individual experiment sections) in five blocks, each block for a different interface level. Between each block, participants filled out the After Scenario, NASA TLX and AttrakDiff questionnaires. At the end of the study, a semi-structured interview was conducted, and participants filled out a separate preference questionnaire. Finally, the participants received a book voucher worth 10 Euros as compensation. Participants were free to take a break between individual blocks and tasks. Overall, the study lasted ˜100 minutes per participant.

Samples of the informed consent form and questionnaires can be found in the appendix (Section A.1).

5.4 Participants

Twenty-six participants volunteered in the study. Three participants had to be excluded due to technical errors (failed tracking or logging). In total, data from twenty three participants (1 female, average age: 26.75 years, =5.3, average height: 179 cm, = 6, 7 users wore glasses, 3 contact lenses, 2 left-handed users) was analysed. All but one user were smartphone owners (one less than a year). Nobody was a user of smartwatches or head-mounted displays. Twenty users had a high interest in technology and strong computer skills (three medium).

Figure 10: Locator Task on Map: BodyRef condition

5.5 Hypotheses

One of the main interests was to investigate if combined display interaction could outperform interaction with individual wearable devices. HHD interaction was included as a baseline and was not expected to be outperformed by the combined interfaces. Hence, the following hypotheses were set up:

- *H1:* HHD will be fastest for all tasks.
- *H2:* BodyRef will be faster than HMD and SW (ideally close to HHD).
- *H3:* BodyRef will result in fewer errors than HMD and SW.
- *H4:* SWRef will be faster than HMD and SW (ideally close to HHD).
- *H5:* SWRef will result in fewer errors than HMD and SW.

5.6 Experiment 1: Locator Task On Map

A common task on mobile mapping applications is to search for an object with certain target attributes [Rei01]. A locator task similar to previous studies involving handheld devices and multi-display environments [GPG+14, RNQ12] was employed. Participants had to find the lowest price label (text size 12 pt) among five labels on a workspace size of 400x225 mm. The workspace size was determined empirically, to still allow direct spatial pointing for the BodyRef condition. While finding the lowest price could easily be solved with other widgets (such as a sortable list view), this task is only

an instance of general locator tasks, which can encompass non-quantifiable attributes such as textual opinions of users, which cannot be sorted automatically. Users conducted ten trials per condition. With 23 participants, five interface levels and 10 trials, there was a total of 23x5x10=1150 trials.

5.6.1 Task Completion Time

The task completion times (TCT, in seconds), for the individual conditions were as follows: HHD (M=15.67, σ=5.45), SW (M=20.60, σ=7.62), HMD (M=18.68, σ=6.45), BodyRef (M=16.57, σ=6.16), SWRef (M=21.05, σ=10.28). A repeated measures ANOVA indicated that there was a significant effect of interface on TCT, F(3.10, 709.65)=42.21, p<.001. The results of post-hoc tests with Bonferroni corrections are depicted in Table 1. Pairs are column-wise (e.g., pair HHD-SW: t=-11.0, p=<.01, d=-.72). Significant differences are highlighted in bold. For all tests, degrees of freedom were 229. To summarize, both HHD and BodyRef were significantly faster than all remaining interfaces with medium to large effect sizes. HMD was significantly faster than both SW and SWRef. There were no significant differences between HHD-BodyRef and SW-SWRef. The smaller standard deviations of HHD, SW and HMD compared to BodyRef and SWRef could be attributed to the longer familiarity of users with touch screen interaction, compared to the novel interfaces introduced in this work.

5.6.2 Errors

From 230 selections, eight false selections were made in the HHD, HMD and BodyRef conditions. In the SW condition, 13 errors have been made, in SWRef, five errors. A Friedman ANOVA indicated no significant effect of interface on errors χ2(4)=4.10, p=.39.

5.6.3 Subjective Workload

The subjective workload scores for individual dimensions, as measured by the NASA TLX, are depicted in Figure 12. A repeated measures ANOVA indicated that there were significant effects of interface on all dimensions. The results of post-hoc tests with Bonferroni corrections indicated significant differences for the dimensions. BodyRef resulted in a higher mental demand than smartwatch (albeit with a small effect size). The handheld condition resulted in lower subjective workload for all other dimensions compared to most other interfaces.

t, p, d	HHD	SW	HMD	BodyRef
HHD	-			
SW	**-11.0, <.01, -.72**	-		
HMD	**-7.4, <.01, -.49**	**3.6, .004, .24**	-	
BodyRef	-2.3, .22, -.15	**8.4, <.01, .56**	**5.1, <.01, .33**	-
SWRef	**-8.8, <.01, -.59**	-1.1, 1.0, -.07	**-4.1, <.01, .27**	**-7.3, <.01, -.48**

Table 1: Test statistics (t-value, p-value, Cohen's d, paired sample t-test with Bonferroni correction) for the map task.

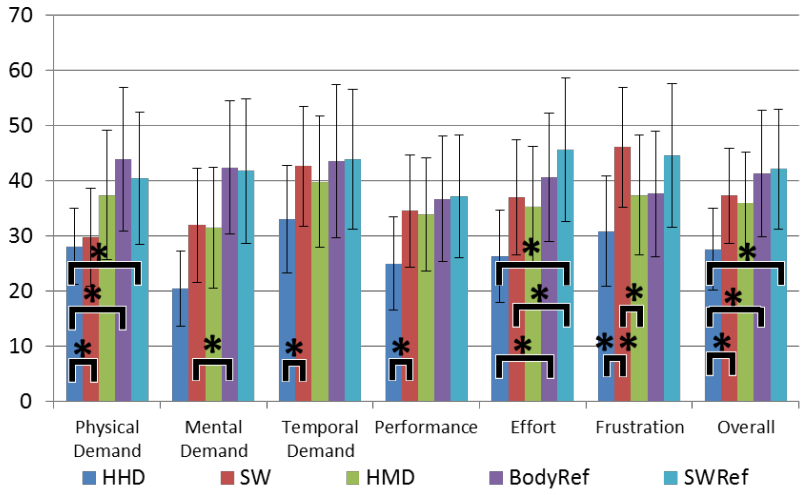

Figure 11: NASA TLX scores for the locator tasks.

5.6.4 User Experience

Results of the After Scenario Questionnaire (seven item Likert scale, 1: totally disagree, 7: totally agree) can be found in Figure 14. Friedman ANOVA indicated significant effect of interface on ease of task ($\chi(4)$=26.65, p<.001), satisfaction with task completion time ($\chi(4)$=9.57, p=.048) and system support ($\chi(4)$=12.20, p=.02). However, Wilcoxon signed rank tests with Bonferroni corrections only indicated a significant difference between HHD and SWRef for ease of task (Z=-3.36, p=.01).

A repeated measures ANOVA indicated that there was a significant effect of interface on Pragmatic Quality (PQ), F(4, 88)=4.05, p<.001 and on Hedonic Quality Stimulation (HQS), F(2.84 , 62.58)=58.26, p<.001. For PQ, results of post-hoc tests with Bonferroni corrections indicated significant differences, as depicted in Figure 15, left.

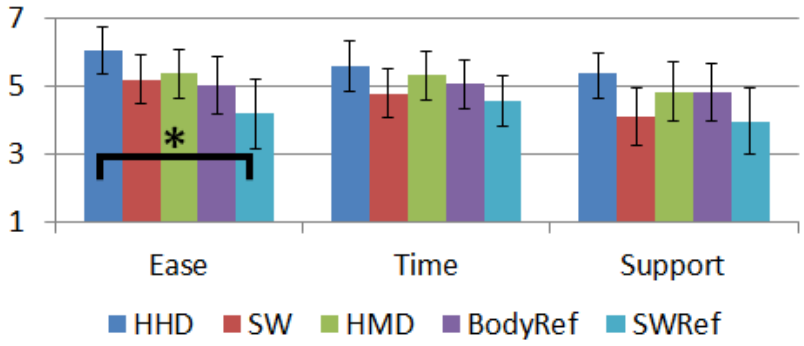

Figure 12: ASQ ratings for locator task (7-point Likert)

Preference ratings (ranking: 1: most preferred 5: least preferred) were as follows. HHD: MD=2, M=1.13, σ=1.13, SW: MD=4, M=3.87, σ=1.10, HMD: MD=2, M=2.78, σ=1.41, BodyRef: MD=4, M=3.22, σ=1.41, SWRef: MD=3, M=3.09, σ=1.38. A Friedman ANOVA indicated that there was a significant effect of interface on preference ($\chi(4)$=19.35, p=.001). Wilcoxon signed rank tests with Bonferroni corrections indicated a significant difference between HHD and SWRef (Z=-4.25, p<.001).

To summarize, for HHD, the ease of task was significantly higher than for SWRef, all interfaces scored slightly below average for pragmatic quality, and only a significant difference between HMD-SWRef could be found (but with a small effect size). For hedonic quality stimulation the HHD and SW interface were rated significantly lower than the other three conditions. HHD was significantly more preferred than SW.

5.7 Experiment 2: 1D Target Acquisition

A discrete 1D pointing task was employed similar to the one used by Zhao et al. [ZSRB14] (Figure 11, right). Participants navigated to a target (green stripe) in each trial using touch input (for HHD, SW, HMD, SWRef) or spatial pointing (BodyRef). Final target selection was confirmed by a touch on the target region in all conditions. The participants were asked to use their index finger to interact with the touch surfaces. For each trial, the task was to scroll the background (HHD, SW, HMD, SWRef) or to move the smartwatch towards the target (BodyRef), until it appeared on the *selection area*. Prior to each trial, participants hit a start button at the center of the screen to ensure a consistent start position and to prevent unintended gestures before scrolling. The target was only revealed after the start button was hit. After successful selection, the target disappeared. For BodyRef,

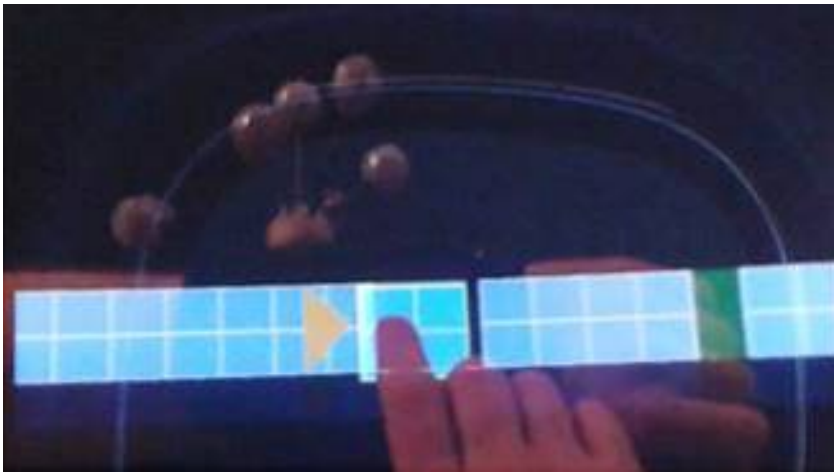

Figure 13: 1D Target Acquisition Task on Map: SWRef condition

participants returned to a neutral start position centered in front of them before the next trial.

Please note that the focus of this experiment is not to derive a new target acquisition model, but rather to get an initial insight into the potential for combined wearable device interaction compared to individual devices. Hence, in the experiment design, all parameters are not varied as one would need for deriving a robust model. Specifically, target width is fixed to 20 mm (0.5*width of the smartwatch), the control window and display window sizes of the individual displays and two target distances (short: 15 cm, long: 30 cm) are used. In addition to interface and target distance, also target direction (same side as hand carrying the smartwatch and opposite side) was introduced as an independent variable, as performance differences in the BodyRef condition were expected. The conditions were blocked by interface. Per condition, each participant conducted eight trials (plus two training trials). With twenty-three participants, five interface levels, two target distances, two directions and eight trials per condition, a total of 23x5x2x2x8=3680 trials were conducted.

5.7.1 Task Completion Time

Task completion times are depicted in Figure 16. A repeated measures ANOVA indicated significant interactions between interface and length, $F(3.23, 592.25)=89.49$, $p<.001$, interface and direction, $F(3.27, 599.15)=5.71$, $p<.001$ and interface, length, direction, $F(2,84, 518.73)=4.58$, $p<.001$. This paragraph reports only on the simple main effects of interface across length and direction. Further details can be found in the appendix (Section A.3). For

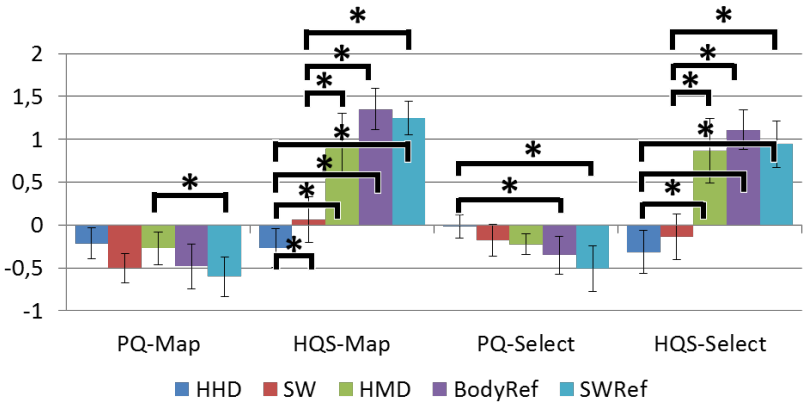

Figure 14: Pragmatic Quality (PQ) and Hedonic Quality Stimulation (HQS) measures (normalized range -2..2) for the locator task (left) and the select task (right).

short distances (15 cm), interface had a significant effect on TCT, $F(3.06, 1122.72)=162.10$, $p<.001$, as well as for long distances (30 cm), $F(3.13, 1147.80)=267.75$, $p<.001$. For selection on the side of the smartwatch (i.e., non-dominant hand side, left for 21 of 23 participants), interface had a significant effect on TCT, $F(3.27, 1201.05)=316.35$, $p<.001$, as well as for selection on the opposite side of the smartwatch (i.e. dominant hand side), $F(3.12, 1145.40)=127.57$, $p<.001$. The results of post-hoc comparisons with Bonferroni correction are depicted in Figure 16. To summarize, HHD was the fastest interface for both directions and distances. BodyRef was significantly faster than all remaining interfaces. No other significant effects of interface on task completion time were found.

5.7.2 Errors

Selection errors occurred when participants tapped outside the target region. The total number of errors (M, σ) for individual interfaces were as follows: HHD: 53 (M=.07, σ=.28), SW: 34 (M=.05, σ=.23), HMD: 223 (M=.30, σ=.77), BodyRef: 258 (M=.35, σ=.78), SWRef: 37 (M=.05, σ=.24). A Friedman ANOVA indicated that there was a significant effect of interface on error count ($\chi(4)=231.68$, $p<.001$). Wilcoxon signed rank tests with Bonferroni corrections indicated significant differences between BodyRef and all interfaces except HMD, as well as between HMD and all interfaces (except BodyRef). No significant effects of direction or length on error rate were identified. To summarize, HMD and BodyRef resulted in a significant higher

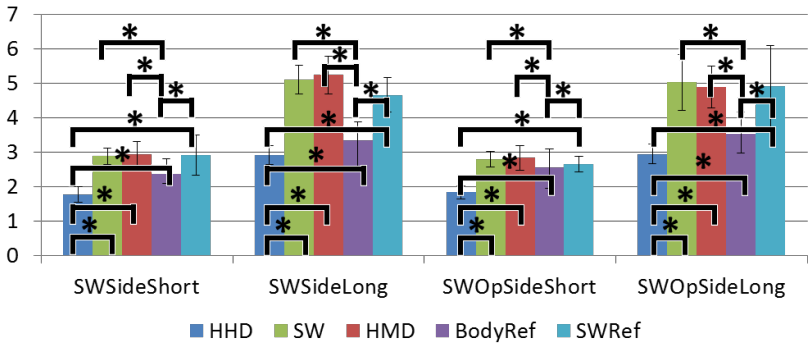

Figure 15: Task completion times (in seconds) for the select task. SWSide: side on which smartwatch was worn, SWOpSide: opposite side.

error rate.

5.7.3 Subjective Workload

The subjective workload scores for individual dimensions, as measured by the NASA TLX, are depicted in Figure 17. A repeated measures ANOVA indicated that there were significant effects of interface on all dimensions, but temporal demand and performance. The results of post-hoc tests with Bonferroni corrections indicated significant differences shown in Figure 17. To summarize, HHD resulted in a lower mental demand than most other conditions (except SW) and in a lower overall demand than all conditions. BodyRef and SWRef resulted in significantly higher physical demands, compared to HHD and HMD (but not SW). Frustration was significantly higher for SW and SWRef compared to HHD.

5.7.4 User Experience

Results of the After Scenario Questionnaire (seven-item Likert scale, 1: totally disagree, 7: totally agree) can be found in Figure 14. Friedman ANOVAs indicated that there were significant effects of interface on ease of task ($\chi(4)$=26.65, p<.001), satisfaction with task completion time ($\chi(4)$=9.57, p=.048) and system support ($\chi(4)$=12.20, p=.02). However, Wilcoxon signed rank tests with Bonferroni corrections only indicated a significant difference between HHD and SWRef for ease of task (Z= -3.36, p=.01).

Pragmatic Quality (PQ) and Hedonic Quality Stimulation (HQ-S), as measured by AttrakDiff, are depicted in Figure 15, right. A repeated measures ANOVA indicated that there was a significant effect of interface on

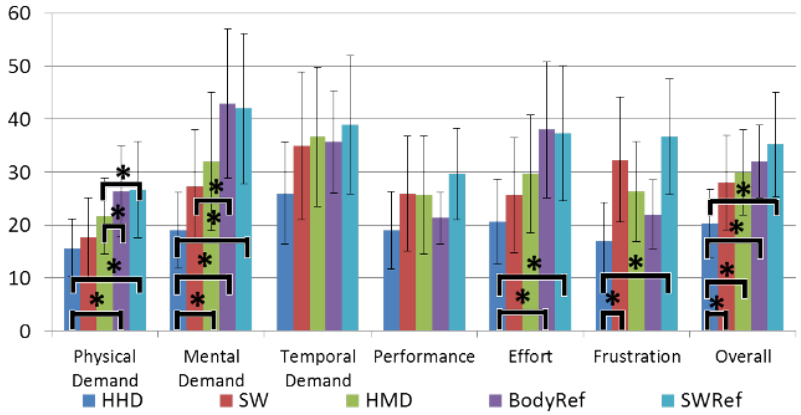

Figure 16: NASA TLX scores for the selection tasks.

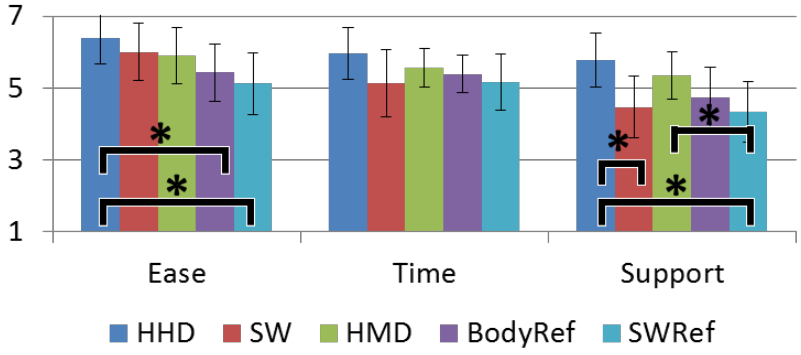

Figure 17: ASQ ratings for select task (7-point Likert)

PQ, F(2.76, 60.69)=4.05, p<.001 and on HQ-S, F(4 , 88)=48.45, p<.001. For PQ, results of post-hoc tests with Bonferroni corrections indicated significant differences as depicted in Figure 15, right.

Preference ratings (ranking: 1: most preferred 5: least preferred) were as follows. HHD: MD=2, M=2.13, σ=1.10, SW: MD=5, M=4.09, σ=1.16, HMD: MD=3, M=2.91, σ=1.24, BodyRef: MD=3, M=2.78, σ=1.54, SWRef: MD=3, M=3.09, σ=1.28. A Friedman ANOVA indicated that there was a significant effect of interface on preference (χ(4)=17.58, p=.001). Wilcoxon signed rank tests with Bonferroni corrections indicated a significant difference between HHD and SWRef task (Z=-4.15, p<.001).

To summarize, HHD scored significantly higher for ease of task and system support compared to BodyRef and SWRef (for system support also compared to SW). As in the locator task, all interfaces scored below average for pragmatic quality. BodyRef and SWRef scored significantly lower than HHD. For hedonic quality stimulation, the HHD and SW interface were rated significantly lower than the other three conditions, as in the locator task. HHD was significantly more preferred than SW.

5.8 Qualitative Feedback

After each task was completed and all forms filled out, users commented on their experience in semi-structured interviews, openly answering questions about their most and least preferred conditions, as well as potentials and limitations of the prototypical MultiFi implementation.

Most participants (21) positively highlighted the *extended view space* given by the combined smartwatch and head-mounted display interfaces. One participant said *"Getting an overview with simple head movements is intuitive and natural."* The same participants generally appreciated the precision given by the smartwatch's touch screen for spatial pointing *"The HMD gives you the overview, and the smartwatch lets you be precise in your selection"*. Five participants pointed out an advantage of MultiFi over HMD-only interaction, highlighting direct interaction and the ability to *"take advantage of proprioception and motion control"*, with another also highlighting the "hands-free" interaction enabled through wearable devices.

In line, participants perceived BodyRef as the fastest condition in both tasks (even though this was not confirmed by objective measurements). Three participants mentioned the potential in the reduced access cost with comments along the lines of *"I don't have to constantly monitor my smartphone."*

Users could see potential applications using multi fidelity interaction. A user said *"This could be useful for presentations. I can keep eye contact with*

my audience, while seeing the slides on the HMD and controlling them with the smartwatch". Another stated that the combination of HMD and spatial pointing with the smartwatch could be applied for an augmented reality room designer. Six participants could imagine MultiFi in medical, industrial or business environments, while others could see it applied in augmented reality games. Some participants highlighted the potential of geo-referenced data being displayed in the HMD and interacted with through the smartwatch, e.g., for public transport schedules or sight-seeing.

The used hardware was a limiting factor for many participants (15). Reasons include the quality of the HMD, the weight of the wearable devices and their form factor, with comments like *"The combined interfaces [SWRef, BodyRef] gave me trouble, because of display quality/weight/form factor."* An interesting point was made by a few users in regard to difficulties when alignment of HMD and smartwatch was required: *"Either I have to look down with my head, which leads to strain on the neck, or I have to hold up my arm, which leads to a tired arm. Usually, when I want to look at a watch, I just need to glance down with my eyes."*

Six participants mentioned the *cost of focus switching*, i.e., accommodation between the different focus depths of HMD, smartwatch and the real world, with comments such as *"I have to focus on three layers, which is overwhelming: HMD, smartwatch and real world."* Nine participants experienced coordination problems across devices. Hence, a suggestion was made by a few candidates to separate input and output rather than combining the screens: *"Pairing the two devices is good, but use one as input, the other as output, not both as output, it is confusing."*

A few users expectedly raised social concerns about wearing the HMD in the first place or about using wide motion control in public, in particular in crowded areas, e.g., *"I could not imagine to use this in a packed bus."*

6 Discussion

After introducing the concept, experimenting with various prototypes and having completed a first user study, this chapter serves to discuss the observations made during this work.

First, the hypotheses proposed in Chapter 5.5 are compared to the outcome of the user study. This is followed by an analysis of verbal user feedback. Finally, Chapter 6.3 summarizes what this means for further development of MultiFi.

6.1 Hypotheses

Returning to the hypotheses after the user study, the following observations have been made: H1 does not hold, as the smartphone-only condition HHD did not significantly outperform the combined smartwatch and head-mounted display interfaces SW and HMD in terms of task completion time. H2 holds, as BodyRef performed significantly faster than the conditions featuring the individual devices alone. SWRef did not perform significantly faster than the other conditions (H4 does not hold). This shows that a combined interface of smartwatch and HMD is indeed capable of both competing with smartphones and providing an advantage over the smartwatch and HMD alone in terms of speed. However, this benefit comes at the cost of lower usability ratings. This effect on usability may be explained by two major sources. First, laboratory equipment heavier than a typical smartwatch or HMD has been used, roughly double the weight of an actual smartwatch or an unaltered HMD. Participants mentioned that they would prefer the interface, had lighter equipment been used. Second, learning a novel interaction technique is challenging, while comparing to an established one. It seems plausible that lighter equipment and more training could mitigate these effects on perceived workload.

Regarding the error rates, for the locator task, no significant differences between conditions can be found. In the selection task, both BodyRef and HMD resulted in significantly higher error rates, compared to all other conditions (H3 does not hold), and SWRef did not perform significantly different compared to SW and HMD (H5 does not hold). For the HMD-only condition, the higher error rate may be caused by the indirect input as well as the discrepancy between the sizes of the output area on the HMD and the smaller input area on the smartwatch, making it harder to judge spatial relations between touch inputs and the information space seen on the HMD. For the BodyRef condition, closer examination showed that an average end-to-end delay from user motion to display update of 154ms ($\sigma = 36$) was caused by the outside-in tracking system and system architecture. A further

video analysis revealed that several participants tapped the screen multiple times when the target came into view, even though they were instructed to be precise in their selection. This may have happened instinctively to mitigate the delayed screen update, prioritizing speed over accuracy. It appears reasonable to assume that future tracking systems can significantly reduce the delay, allowing more precise physical pointing.

6.2 User Feedback

The semi-structured interviews at the end and notes taken during testing offered a fresh perspective on the development of MultiFi. As expected, most users preferred the HHD condition for both tasks, because of its familiarity, largest touch input area and most comfort in usability.

The BodyRef condition was often named as the favorite (or second favorite after HHD) condition. Participants highlighted the intuitive way to *"first get an overview by moving the head and then selecting precisely with the smart watch"*, in particular for the locator task. For both tasks, some participants mentioned that *"knowing where you move, before you move, makes it easier than other conditions."* Some candidates pointed out that they *"would prefer to just point with [their] fingers or eyes"* rather than tapping the smartwatch to confirm a selection.

SW-only was considered to be the least preferred condition for both tasks, due to cumbersome interaction on the small touch screen. In the locator task, it was hard to get an overview, as zooming out too much led to the labels becoming unreadable, while zooming in far enough to read the levels made it hard to orientate oneself. In the selection task, a lot of scrolling was required to reach the target, and then some participants mentioned that they felt like they nearly missed it when it finally arrived. Some said something along the lines of *"I was not sure if I was scrolling in the right direction."*

The HMD condition received generally positive impressions, in particular citing the "lean-back" experience, coming from the ability to just lean back and have the arm in a rested position while scrolling. Some participants said that *"[using the smartwatch as a touchpad] is better than Google Glass."*

Interestingly, the SWRef condition did not perform better than the individual device conditions, for both tasks, despite being essentially the SW-only condition with the additional extended screen space, which benefited the BodyRef condition. For the locator task, some participants mentioned that they had difficulties refocusing between the smartwatch (focus plane at ˜40cm) and the HMD display (˜300cm). While the refocusing also has to happen for the BodyRef condition, the larger impact of the switching may have to do with there being requirement for only one focus switch in the

BodyRef condition (first get the overview, then focus switch to smartwatch and, finally, select), while, in SWRef, potentially more focus switches may have been performed by participants. For the selection tasks, some participants claimed to benefit from the extended screen space (*"I can see the target coming in my peripheral view, so I do not scroll too far like in SW-only"*), while others said that their performance was actually hindered by the HMD, rather than helped (compare with Section 5.8).

Despite the rather unspectacular performance of SWRef, qualitative participant feedback indicates that smartwatch referenced display space extension could be beneficial, if the visual fidelity of the HMD and costs of display switching is considered in the design process.

6.3 Revisiting MultiFi

The study results show through both objective measurements and subjective user feedback that there is potential found in the concept of MultiFi. The BodyRef condition was able to go head to head with the smartphone in both the locator and the selection task and performed significantly better than the wearable devices on their own. Users complimented the intuitive method to interact through overview and selection, and users could see the benefits of the reduced *access cost*, as well as *direct interaction* with haptic feedback through the smartwatch, as opposed to less precise mid-air interaction based on depth sensors found in other approaches. However, these benefits come at the cost of higher physical and mental workload, and large arm movements may be a concern in crowded places.

The tradeoff between workload, efficiency and social acceptance in completing tasks suggest, that *dynamic alignment* is a key concept to support a broad range of mobile scenarios. It allows a user to choose the ideal mode based on the current situation and develop personal preferences.

The motion-heavy body-aligned mode may benefit from focusing on head movements stronger than on arm movements, designing interfaces in such a way that arm movements are minimized. The feedback on the HMD-only condition indicates that the side-by-side mode can be a valuable asset for crowded places or when a user desires to casually browse larger information spaces with lower accuracy requirements. User feedback such as *"I would like a hybrid mode between SWRef and BodyRef"*suggests that users would be open to this idea. Further user studies need to be conducted to show user behaviour when presented with various ways of changing alignment modes on the fly in order to complete tasks.

However, the SWRef condition shows that mere screen space extension by itself is not enough to benefit the user, and that careful thought needs to

be put in designing widgets for multiple devices in order to better overcome interaction seams. Large differences in focus planes seem to have significant impact on coordination cost across displays. The same can be said of overloading the peripheral view with too much information, unintendingly distracting users from the outside world. A possible solution for the focus issue could be to use HMDs that have a focus plane closer to the ideal viewing distance of a smartwatch. The information overload may be mitigated by reducing the information displayed on the HMD, when in device-aligned mode, e.g., for a map by only showing points of interest, rather than fully detailed maps, while only the touch device shows more details (similar to the arm clipboard).

7 Conclusion and Future Work

This last chapter provides a conclusion to this work, summarizing the most important findings and challenges emerging from the development as well as the user study. Finally, potential topics for future work are listed, highlighting challenges that require attention in order to make MultiFi a viable solution for mobile interaction on the go.

7.1 Conclusion

While two new device types on the verge of mass market introduction, smartwatch and HMD, struggle to provide the usability of the ubiquitous smartphone and tablet, the combination of these devices could show a significant improvement.

This work introduced *MultiFi*, a novel multi fidelity interface focusing on the above mentioned wearbles and exploring ways to minimize the interaction seams in interaction with multiple devices by dynamic alignment. At first, the challenges of creating such an interface were discussed, highlighting design factors such as spatial reference frames, fidelity concerns, direct vs. indirect input, continuity and social acceptability.

A prototype was implemented as a proof of concept, with implementation details given and some examples described in-depth, e.g., a map taking advantage of extended screen space, a focus+context list and a full screen virtual keyboard on a smartphone. Practical use of such applications has been demonstrated in a house hunting scenario.

The results of the user study show that this approach can outperform interaction with single wearable devices in terms of task completion time, albeit with higher workload. The user study also produced qualitative feedback from semi-structured interviews that may prove useful for future development of the MultiFi concept. Amongst other statements, users could see the benefit of multi-fidelity interfaces in terms of access cost. Feedback also showed that there is room for improvement in regards to focus switching, dealing with information overload and careful design in order to optimally leverage the different alignment modes.

7.2 Future Work

The subject opens up a quite interesting design space that was only initially explored within the scope of this work. Future work can expand in multiple directions, for example, making prototypes available in a true mobile environment, using real smartwatches, inside-out tracking and hosting the

central server on the smartphone. This would also facilitate the inclusion of geo-referenced data.

Work can also be done in regard to providing a fleshed out framework, providing developers with unified tools to create multi-fidelity applications with a similar ease as for current smartphones.

Another interesting subject for future research is to enable multiple users to interact with each other both locally and remotely through MultiFi. For example, how can one handle tracked smartwatches of multiple users in order to share information intuitively.

Yet, in order to fully benefit from the potential of MultiFi, future work needs to address the challenges encountered during this work. For instance, optimizing the distribution of information across devices can avoid users being overwhelmed by frequent focus switches. We also suggest the exploration of intuitive methods to seamlessly switch between alignment modes.

A Appendix

Included are the questionnaires and forms used in the user study, and detailed statistics for both tasks.

A.1 Questionnaires and Forms

The following pages contain samples of the informed consent form, the background questionnaire and the post questionnaire. The standardized questionnaires ASQ [Lew91], NASA TLX [HS88] and AttrakDiff [HBK03] are not included.

USER NUMBER | **CODE** | **DATE**

INFORMED CONSENT FORM

PRINCIPAL INVESTIGATOR. Jens Grubert (grubert@icg.tugraz.at)

INTRODUCTION. You are invited to take part in a research study. Before you decide to be part of this study, you need to understand the risks and benefits. Your participation in this study is voluntary, and you are free to withdraw the study at any time, without prejudice to you. If you have any questions or concerns about this experiment, or its implementation, we will be happy to discuss them with you.

PURPOSE. We are carrying out research to investigate the usage of novel wearable user interfaces.

PROCEDURE. We will ask you to interact with several user interfaces. You will also be asked to rate the user interfaces. Remember that the system is being evaluated – not you. You will be photographed and videoed during the experiment.

BENEFITS. The results of this experiment will help to get insight into usage patterns of novel wearable user interfaces.

CONFIDENTIALITY. The data collected from your participation will be kept confidential and anonymous, and will not be released to anyone except to the researchers directly involved in this project.

By signing this consent form, you affirm that you have read this informed consent form, the study has been explained to you, your questions have been answered, and you agree to take part in this study. You do not give up any legal rights by signing this informed consent form. You will receive a copy of this consent form.

_____ _____ _____

Participant (Print name) Signature Date

By signing underneath you authorize publication of photographs, videos, sound recordings or other materials taken from this study for scientific purposes. You understand that TU Graz will own the copyright to these materials and may grant permission for use of these materials for teaching, research, scientific meetings, other professional publications. These materials may appear in print and online.

_____ _____

Signature Date

Background Questionnaire

* Required

1. **User number** *
   to be filled in by study supervisor

2. **Sex** *
   Mark only one oval.
   - female
   - male

3. **Nationality** *

4. **Height (in cm)** *

5. **Age** *

6. **Which is your dominant hand?** *
   Mark only one oval.
   - left
   - right
   - both

7. **Do you have problems with your vision (near- or far sighted, color blindness)?** *
   Mark only one oval.
   - Yes
   - No

8. **If so, which problems?**

9. **If so, which type of optical aid do you use?**

10. **If so, what are your diopter numbers?**

11. **On average how many hours do you play video games per week ?** *

Mark only one oval per row.

	never	0-1	1-5	5-10	10-15	15-20	>20
Hours							

12. **Technology** *

Mark only one oval per row.

	Very low	Low	Medium	High	Very High
How would you rate your general computer skills?					
How would you rate your general interest in technology?					

13. **How would you describe your knowledge about ...** *

Mark only one oval per row.

	Never heard of it	Heard about it in the news	I am familiar with basic concepts	Used it more than once	I am a regular user or professional
Augmented Reality (AR)					
Smartwatches					
Head-mounted displays					

14. **Do you use a smartphone or tablet?** *

Mark only one oval.

- Yes
- No

15. **If yes, which model(s)?**

_____

16. **If yes, for how long you already use smartphones (in months) ?**

Mark only one oval.

- < 3
- 3-12
- 13-24
- >24

17. **Do you use a smartwatch?** *

Mark only one oval.

- Yes
- No

18. **If yes, which model(s)?**

_____

19. **If yes, for how long do you already use smartwatches (in months)?**
Mark only one oval.

- < 3
- 3-12
- 12-24
- > 24

20. **Do you use a head-mounted display (HMD, e.g. Google Glass)?** *
Mark only one oval.

- Yes
- No

21. **If yes, which model(s)?**

_____

22. **If yes, for how long do you already use head-mounted displays (in months)?**
Mark only one oval.

- < 3
- 3-12
- 13-24
- > 24

Post

* Required

1. **User number** *

   to be filled in by study supervisor

2. **Please sort the interfaces for the *selection task* according to your personal preference** *

   Mark only one oval per row.

	1 (most preferred)	2	3	4	5 (least preferred)
Smartphone Only					
Smartwatch Only					
Head Mounted Display Only					
Smartwatch + HMD Hybrid					
Body Referenced (on the table)					

3. **Please sort the interfaces for the *map task* according to your personal preference** *

   Mark only one oval per row.

	1 (most preferred)	2	3	4	5 (least preferred)
Smartphone Only					
Smartwatch Only					
Head Mounted Display Only					
Smartwatch + HMD Hybrid					
Body Referenced (on the table)					

4. **Please sort the interfaces according to your personal preference** *

   Mark only one oval per row.

	1 (most preferred)	2	3	4	5 (least preferred)
Smartphone Only					
Smartwatch Only					
Head Mounted Display Only					
Smartwatch + HMD Hybrid					
Body Referenced (on the table)					

5. **Additional remarks**

A.2 Detailed Statistics for Experiment 1: Locator Task on Map

Mauchly's Test of Sphericity[b]

Measure:TCT

Within Subjects Effect	Mauchly's W	Approx. Chi-Square	df	Sig.	Epsilon[a]		
					Greenhouse-Geisser	Huynh-Feldt	Lower-bound
interface	,617	109,837	9	,000	,775	,787	,250

Tests the null hypothesis that the error covariance matrix of the orthonormalized transformed dependent variables is proportional to an identity matrix.

a. May be used to adjust the degrees of freedom for the averaged tests of significance. Corrected tests are displayed in the Tests of Within-Subjects Effects table.
b. Design: Intercept
Within Subjects Design: interface

Tests of Within-Subjects Effects

Measure:TCT

Source		Type III Sum of Squares	df	Mean Square	F	Sig.	Partial Eta Squared	Noncent. Parameter	Observed Power[a]
interface	Sphericity Assumed	4978,603	4	1244,651	42,206	,000	,156	168,824	1,000
	Greenhouse-Geisser	4978,603	3,099	1606,578	42,206	,000	,156	130,792	1,000
	Huynh-Feldt	4978,603	3,146	1582,387	42,206	,000	,156	132,791	1,000
	Lower-bound	4978,603	1,000	4978,603	42,206	,000	,156	42,206	1,000
Error(interface)	Sphericity Assumed	27012,729	916	29,490					
	Greenhouse-Geisser	27012,729	709,645	38,065					
	Huynh-Feldt	27012,729	720,494	37,492					
	Lower-bound	27012,729	229,000	117,960					

a. Computed using alpha = ,05

The p-values in the following table are not Bonferroni corrected. Bonferroni corrected values are p-value*0.1.

Paired Samples Test

		Paired Differences					t	df	Sig. (2-tailed)
		Mean	Std. Deviation	Std. Error Mean	95% Confidence Interval of the Difference Lower	Upper			
Pair 1	HHD - SW	-4,66661	6,43000	,42398	-5,50201	-3,83120	-11,007	229	,000
Pair 2	HHD - HMD	-3,00882	6,16431	,40646	-3,80970	-2,20793	-7,402	229	,000
Pair 3	HHD - BodyRef	-,89360	5,87902	,38765	-1,65742	-,12979	-2,305	229	,022
Pair 4	HHD - SWRef	-5,37769	9,18462	,60562	-6,57098	-4,18440	-8,880	229	,000
Pair 5	SW - HMD	1,65779	6,99779	,46142	,74862	2,56696	3,593	229	,000
Pair 6	SW - BodyRef	3,77300	6,77863	,44697	2,89231	4,65370	8,441	229	,000
Pair 7	SW - SWRef	-,71108	9,68903	,63888	-1,96991	,54774	-1,113	229	,267
Pair 8	HMD - BodyRef	2,11521	6,32419	,41700	1,29356	2,93687	5,072	229	,000
Pair 9	HMD - SWRef	-2,36887	8,71125	,57440	-3,50066	-1,23708	-4,124	229	,000
Pair 10	BodyRef - SWRef	-4,48409	9,31967	,61452	-5,69492	-3,27325	-7,297	229	,000

A.2.1 Errors

Ranks

	Mean Rank
HHD	3,00
SW	2,95
HMD	3,00
BodyRef	3,00
SWRef	3,04

Test Statistics[a]

N	230
Chi-Square	4,099
df	4
Asymp. Sig.	,393

a. Friedman Test

The p-values in the following table are not Bonferroni corrected. Bonferroni corrected values are p-value*0.1.

Test Statistics[d]

	SW - HHD	HMD - HHD	BodyRef - HHD	SWRef - HHD	HMD - SW	BodyRef - SW	SWRef - SW	BodyRef - HMD	SWRef - HMD	SWRef - BodyRef
Z	-1,147[a]	,000[b]	,000[b]	-,832[c]	-1,091[c]	-1,091[c]	-2,000[c]	,000[b]	-,832[c]	-,832[c]
Asymp. Sig. (2-tailed)	,251	1,000	1,000	,405	,275	,275	,046	1,000	,405	,405

a. Based on positive ranks.
b. The sum of negative ranks equals the sum of positive ranks.
c. Based on negative ranks.
d. Wilcoxon Signed Ranks Test

A.2.2 Subjective Workload

interfaces: 1: HHD, 2: SW, 3: HMD, 4: BodyRef, 5: SWRef

md: mental demand, pd: physical demand, td: temporal demand, p: performance, e: effort, f: frustration, o: overall.

Mauchly's Test of Sphericity[b]

Within Subjects Effect	Measure	Mauchly's W	Approx. Chi-Square	df	Sig.	Epsilon[a]		
						Greenhouse-Geisser	Huynh-Feldt	Lower-bound
interface	md	,222	30,728	9	,000	,543	,605	,250
	pd	,504	14,000	9	,123	,790	,939	,250
	td	,428	17,334	9	,044	,697	,808	,250
	p	,423	17,578	9	,041	,756	,890	,250
	e	,241	29,094	9	,001	,574	,644	,250
	f	,452	16,218	9	,063	,734	,860	,250
	o	,459	15,888	9	,070	,718	,837	,250

Tests the null hypothesis that the error covariance matrix of the orthonormalized transformed dependent variables is proportional to an identity matrix.

a. May be used to adjust the degrees of freedom for the averaged tests of significance. Corrected tests are displayed in the Tests of Within-Subjects Effects table.
b. Design: Intercept
Within Subjects Design: interface

Univariate Tests

Source	Measure		Type III Sum of Squares	df	Mean Square	F	Sig.	Partial Eta Squared	Noncent. Parameter	Observed Power[a]
interface	md	Sphericity Assumed	4281,304	4	1070,326	5,854	,000	,210	23,417	,979
		Greenhouse-Geisser	4281,304	2,173	1969,900	5,854	,004	,210	12,724	,872
		Huynh-Feldt	4281,304	2,420	1768,882	5,854	,003	,210	14,170	,899
		Lower-bound	4281,304	1,000	4281,304	5,854	,024	,210	5,854	,638
	pd	Sphericity Assumed	7449,130	4	1862,283	7,879	,000	,264	31,514	,997
		Greenhouse-Geisser	7449,130	3,162	2356,019	7,879	,000	,264	24,910	,989
		Huynh-Feldt	7449,130	3,754	1984,282	7,879	,000	,264	29,577	,996
		Lower-bound	7449,130	1,000	7449,130	7,879	,010	,264	7,879	,765
	td	Sphericity Assumed	1864,348	4	466,087	3,087	,020	,123	12,349	,791
		Greenhouse-Geisser	1864,348	2,786	669,079	3,087	,037	,123	8,602	,672
		Huynh-Feldt	1864,348	3,231	576,934	3,087	,029	,123	9,976	,721
		Lower-bound	1864,348	1,000	1864,348	3,087	,093	,123	3,087	,390
	p	Sphericity Assumed	2243,478	4	560,870	3,074	,020	,123	12,296	,789
		Greenhouse-Geisser	2243,478	3,024	741,915	3,074	,033	,123	9,295	,697
		Huynh-Feldt	2243,478	3,560	630,239	3,074	,025	,123	10,942	,751
		Lower-bound	2243,478	1,000	2243,478	3,074	,093	,123	3,074	,389
	e	Sphericity Assumed	4732,609	4	1183,152	6,217	,000	,220	24,868	,985
		Greenhouse-Geisser	4732,609	2,295	2061,883	6,217	,003	,220	14,270	,905
		Huynh-Feldt	4732,609	2,578	1836,028	6,217	,002	,220	16,025	,929
		Lower-bound	4732,609	1,000	4732,609	6,217	,021	,220	6,217	,664
	f	Sphericity Assumed	3481,304	4	870,326	4,036	,005	,155	16,142	,898
		Greenhouse-Geisser	3481,304	2,937	1185,316	4,036	,011	,155	11,852	,813
		Huynh-Feldt	3481,304	3,439	1012,393	4,036	,007	,155	13,877	,859
		Lower-bound	3481,304	1,000	3481,304	4,036	,057	,155	4,036	,484
	o	Sphericity Assumed	3100,085	4	775,021	7,476	,000	,254	29,905	,996
		Greenhouse-Geisser	3100,085	2,872	1079,264	7,476	,000	,254	21,475	,978
		Huynh-Feldt	3100,085	3,349	925,573	7,476	,000	,254	25,040	,989
		Lower-bound	3100,085	1,000	3100,085	7,476	,012	,254	7,476	,743
Error(interface)	md	Sphericity Assumed	16088,696	88	182,826					
		Greenhouse-Geisser	16088,696	47,814	336,485					
		Huynh-Feldt	16088,696	53,248	302,149					
		Lower-bound	16088,696	22,000	731,304					
	pd	Sphericity Assumed	20800,870	88	236,374					
		Greenhouse-Geisser	20800,870	69,558	299,042					
		Huynh-Feldt	20800,870	82,590	251,858					
		Lower-bound	20800,870	22,000	945,494					
	td	Sphericity Assumed	13285,652	88	150,973					
		Greenhouse-Geisser	13285,652	61,302	216,726					
		Huynh-Feldt	13285,652	71,092	186,879					
		Lower-bound	13285,652	22,000	603,893					
	p	Sphericity Assumed	16056,522	88	182,460					
		Greenhouse-Geisser	16056,522	66,526	241,358					
		Huynh-Feldt	16056,522	78,314	205,028					
		Lower-bound	16056,522	22,000	729,842					
	e	Sphericity Assumed	16747,391	88	190,311					
		Greenhouse-Geisser	16747,391	50,496	331,656					
		Huynh-Feldt	16747,391	56,708	295,327					
		Lower-bound	16747,391	22,000	761,245					
	f	Sphericity Assumed	18978,696	88	215,667					
		Greenhouse-Geisser	18978,696	64,615	293,722					
		Huynh-Feldt	18978,696	75,651	250,871					
		Lower-bound	18978,696	22,000	862,668					
	o	Sphericity Assumed	9122,549	88	103,665					
		Greenhouse-Geisser	9122,549	63,193	144,360					
		Huynh-Feldt	9122,549	73,686	123,803					
		Lower-bound	9122,549	22,000	414,661					

a. Computed using alpha = ,05

Pairwise Comparisons

Measure	(I) interface	(J) interface	Mean Difference (I-J)	Std. Error	Sig.[a]	95% Confidence Interval for Difference[a]	
						Lower Bound	Upper Bound
md	1	2	-1,739	3,137	1,000	-11,524	8,046
		3	-9,348	4,348	,428	-22,908	4,212
		4	-15,870	5,594	,096	-33,315	1,576
		5	-12,391	5,097	,236	-28,287	3,504
	2	1	1,739	3,137	1,000	-8,046	11,524
		3	-7,609	2,963	,176	-16,851	1,634
		4	-14,130*	4,318	,035	-27,596	-,665
		5	-10,652	4,382	,237	-24,318	3,014
	3	1	9,348	4,348	,428	-4,212	22,908
		2	7,609	2,963	,176	-1,634	16,851
		4	-6,522	3,006	,411	-15,896	2,853
		5	-3,043	2,944	1,000	-12,227	6,140
	4	1	15,870	5,594	,096	-1,576	33,315
		2	14,130*	4,318	,035	,665	27,596
		3	6,522	3,006	,411	-2,853	15,896
		5	3,478	2,939	1,000	-5,689	12,646
	5	1	12,391	5,097	,236	-3,504	28,287
		2	10,652	4,382	,237	-3,014	24,318
		3	3,043	2,944	1,000	-6,140	12,227
		4	-3,478	2,939	1,000	-12,646	5,689
pd	1	2	-11,522*	3,631	,044	-22,847	-,197
		3	-11,087	3,837	,085	-23,052	,879
		4	-21,957*	5,314	,004	-38,529	-5,384
		5	-21,304*	4,852	,002	-36,436	-6,173
	2	1	11,522*	3,631	,044	,197	22,847
		3	,435	3,250	1,000	-9,702	10,572
		4	-10,435	4,746	,387	-25,236	4,366
		5	-9,783	4,200	,294	-22,880	3,315
	3	1	11,087	3,837	,085	-,879	23,052
		2	-,435	3,250	1,000	-10,572	9,702
		4	-10,870	4,453	,232	-24,757	3,018
		5	-10,217	5,476	,755	-27,296	6,862
	4	1	21,957*	5,314	,004	5,384	38,529
		2	10,435	4,746	,387	-4,366	25,236
		3	10,870	4,453	,232	-3,018	24,757
		5	,652	5,033	1,000	-15,043	16,348

	5	1	21,304*	4,852	,002	6,173	36,436
		2	9,783	4,200	,294	-3,315	22,880
		3	10,217	5,476	,755	-6,862	27,296
		4	-,652	5,033	1,000	-16,348	15,043
td	1	2	-9,565*	2,571	,012	-17,585	-1,546
		3	-6,739	3,754	,864	-18,447	4,969
		4	-10,435	4,869	,434	-25,620	4,751
		5	-10,870	4,142	,155	-23,789	2,050
	2	1	9,565*	2,571	,012	1,546	17,585
		3	2,826	3,172	1,000	-7,067	12,719
		4	-,870	4,094	1,000	-13,639	11,900
		5	-1,304	2,969	1,000	-10,565	7,956
	3	1	6,739	3,754	,864	-4,969	18,447
		2	-2,826	3,172	1,000	-12,719	7,067
		4	-3,696	3,628	1,000	-15,011	7,620
		5	-4,130	3,185	1,000	-14,064	5,803
	4	1	10,435	4,869	,434	-4,751	25,620
		2	,870	4,094	1,000	-11,900	13,639
		3	3,696	3,628	1,000	-7,620	15,011
		5	-,435	3,281	1,000	-10,666	9,797
	5	1	10,870	4,142	,155	-2,050	23,789
		2	1,304	2,969	1,000	-7,956	10,565
		3	4,130	3,185	1,000	-5,803	14,064
		4	,435	3,281	1,000	-9,797	10,666
p	1	2	-9,565*	2,684	,017	-17,937	-1,194
		3	-8,913	3,556	,201	-20,003	2,177
		4	-11,739	4,213	,108	-24,878	1,400
		5	-12,174	3,949	,054	-24,490	,143
	2	1	9,565*	2,684	,017	1,194	17,937
		3	,652	4,348	1,000	-12,908	14,212
		4	-2,174	3,848	1,000	-14,174	9,826
		5	-2,609	5,009	1,000	-18,230	13,012
	3	1	8,913	3,556	,201	-2,177	20,003
		2	-,652	4,348	1,000	-14,212	12,908
		4	-2,826	3,999	1,000	-15,298	9,646
		5	-3,261	3,523	1,000	-14,249	7,727
	4	1	11,739	4,213	,108	-1,400	24,878
		2	2,174	3,848	1,000	-9,826	14,174
		3	2,826	3,999	1,000	-9,646	15,298
		5	-,435	4,275	1,000	-13,766	12,897
	5	1	12,174	3,949	,054	-,143	24,490
		2	2,609	5,009	1,000	-13,012	18,230
		3	3,261	3,523	1,000	-7,727	14,249

		4	,435	4,275	1,000	-12,897	13,766
e	1	2	-10,652	3,505	,060	-21,583	,278
		3	-8,913	3,414	,160	-19,561	1,735
		4	-14,348*	4,279	,029	-27,694	-1,002
		5	-19,348*	4,438	,003	-33,189	-5,507
	2	1	10,652	3,505	,060	-,278	21,583
		3	1,739	4,452	1,000	-12,147	15,625
		4	-3,696	3,255	1,000	-13,847	6,456
		5	-8,696*	2,480	,020	-16,429	-,963
	3	1	8,913	3,414	,160	-1,735	19,561
		2	-1,739	4,452	1,000	-15,625	12,147
		4	-5,435	4,959	1,000	-20,902	10,033
		5	-10,435	5,701	,808	-28,215	7,346
	4	1	14,348*	4,279	,029	1,002	27,694
		2	3,696	3,255	1,000	-6,456	13,847
		3	5,435	4,959	1,000	-10,033	20,902
		5	-5,000	3,143	1,000	-14,804	4,804
	5	1	19,348*	4,438	,003	5,507	33,189
		2	8,696*	2,480	,020	,963	16,429
		3	10,435	5,701	,808	-7,346	28,215
		4	5,000	3,143	1,000	-4,804	14,804
f	1	2	-15,217*	2,855	,000	-24,121	-6,314
		3	-6,522	3,590	,829	-17,719	4,675
		4	-6,739	4,441	1,000	-20,590	7,112
		5	-13,696	4,852	,099	-28,827	1,436
	2	1	15,217*	2,855	,000	6,314	24,121
		3	8,696*	2,780	,049	,025	17,366
		4	8,478	4,473	,712	-5,471	22,427
		5	1,522	4,874	1,000	-13,680	16,724
	3	1	6,522	3,590	,829	-4,675	17,719
		2	-8,696*	2,780	,049	-17,366	-,025
		4	-,217	5,015	1,000	-15,857	15,422
		5	-7,174	5,125	1,000	-23,158	8,811
	4	1	6,739	4,441	1,000	-7,112	20,590
		2	-8,478	4,473	,712	-22,427	5,471
		3	,217	5,015	1,000	-15,422	15,857
		5	-6,957	4,509	1,000	-21,019	7,106
	5	1	13,696	4,852	,099	-1,436	28,827
		2	-1,522	4,874	1,000	-16,724	13,680
		3	7,174	5,125	1,000	-8,811	23,158
		4	6,957	4,509	1,000	-7,106	21,019
o	1	2	-9,696*	2,361	,005	-17,060	-2,331
		3	-8,449	2,745	,055	-17,010	,111

		4	-13,746*	4,090	,028	-26,504	-,989
		5	-14,558*	3,519	,004	-25,532	-3,584
	2	1	9,696*	2,361	,005	2,331	17,060
		3	1,246	2,215	1,000	-5,660	8,153
		4	-4,051	2,833	1,000	-12,887	4,785
		5	-4,862	2,564	,711	-12,859	3,135
	3	1	8,449	2,745	,055	-,111	17,010
		2	-1,246	2,215	1,000	-8,153	5,660
		4	-5,297	3,240	1,000	-15,401	4,807
		5	-6,109	3,039	,568	-15,586	3,369
	4	1	13,746*	4,090	,028	,989	26,504
		2	4,051	2,833	1,000	-4,785	12,887
		3	5,297	3,240	1,000	-4,807	15,401
		5	-,812	2,947	1,000	-10,003	8,380
	5	1	14,558*	3,519	,004	3,584	25,532
		2	4,862	2,564	,711	-3,135	12,859
		3	6,109	3,039	,568	-3,369	15,586
		4	,812	2,947	1,000	-8,380	10,003

Based on estimated marginal means

a. Adjustment for multiple comparisons: Bonferroni.

*. The mean difference is significant at the ,05 level.

A.2.3 User Experience

A.2.3.1 After Scenario Questionnaire

A.2.3.1.1 Ease of Use

Ranks

	Mean Rank
easeHHD	3,91
easeSW	2,93
easeHMD	3,30
easeBodyRef	2,91
easeSWRef	1,93

Test Statistics[a]

N	23
Chi-Square	25,649
df	4
Asymp. Sig.	,000

a. Friedman Test

The p-values in the following table are not Bonferroni corrected. Bonferroni corrected values are p-value*0.1.

Test Statistics[c]

	easeSW - easeHHD	easeHMD - easeHHD	easeBodyRef - easeHHD	easeSWRef - easeHHD	easeHMD - easeSW	easeBodyRef - easeSW	easeSWRef - easeSW	easeBodyRef - easeHMD	easeSWRef - easeHMD	easeSWRef - easeBodyRef
Z	-2,391[a]	-1,843[a]	-2,515[a]	-3,356[a]	-,674[b]	-,679[a]	-2,527[a]	-1,137[a]	-2,734[a]	-2,614[a]
Asymp. Sig. (2-tailed)	,017	,065	,012	,001	,500	,497	,012	,256	,006	,009

a. Based on positive ranks.
b. Based on negative ranks.
c. Wilcoxon Signed Ranks Test

A.2.3.1.2 Satisfaction with Task Completion Time

Ranks

	Mean Rank
timeHHD	3,54
timeSW	2,59
timeHMD	3,30
timeBodyRef	3,04
timeSWRef	2,52

Test Statistics[a]

N	23
Chi-Square	9,570
df	4
Asymp. Sig.	,048

a. Friedman Test

The p-values in the following table are not Bonferroni corrected. Bonferroni corrected values are p-value*0.1.

Test Statistics[c]

	timeSW - timeHHD	timeHMD - timeHHD	timeBodyRef - timeHHD	timeSWRef - timeHHD	timeHMD - timeSW	timeBodyRef - timeSW	timeSWRef - timeSW	timeBodyRef - timeHMD	timeSWRef - timeHMD	timeSWRef - timeBodyRef
Z	-2,738[a]	-,700[a]	-1,930[a]	-2,680[a]	-1,395[b]	-1,052[b]	-,611[a]	-,956[a]	-1,929[a]	-1,977[a]
Asymp. Sig. (2-tailed)	,006	,484	,054	,007	,163	,293	,541	,339	,054	,048

a. Based on positive ranks.
b. Based on negative ranks.
c. Wilcoxon Signed Ranks Test

A.2.3.1.3 Satisfaction with System Support

Ranks

	Mean Rank
supportHHD	3,70
supportSW	2,50
supportHMD	3,26
supportBodyRef	3,07
supportSWRef	2,48

Test Statistics[a]

N	23
Chi-Square	12,203
df	4
Asymp. Sig.	,016

a. Friedman Test

The p-values in the following table are not Bonferroni corrected. Bonferroni corrected values are p-value*0.1.

Test Statistics[c]

	supportSW - supportHHD	supportHMD - supportHHD	supportBody Ref - supportHHD	support SWRef - supportHHD	supportHMD - supportSW	supportBody Ref - supportSW	support SWRef - supportSW	supportBody Ref - supportHMD	support SWRef - supportHMD	support SWRef - supportBody Ref
Z	-2,654[a]	-1,290[a]	-1,930[a]	-2,783[a]	-1,766[b]	-1,747[b]	-,152[a]	-,058[b]	-1,904[a]	-1,897[a]
Asymp. Sig. (2-tailed)	,008	,197	,054	,005	,077	,081	,879	,954	,057	,058

a. Based on positive ranks.
b. Based on negative ranks.
c. Wilcoxon Signed Ranks Test

A.2.3.2 Pragmatic Quality (PQ) and Hedonic Quality Stimulation (HQS)

interfaces: 1: HHD, 2: SW, 3: HMD, 4: BodyRef, 5: SWRef

Mauchly's Test of Sphericity[b]

Within Subjects Effect	Measure	Mauchly's W	Approx. Chi-Square	df	Sig.	Epsilon[a]		
						Greenhouse-Geisser	Huynh-Feldt	Lower-bound
interface	pq	,472	15,321	9	,083	,721	,842	,250
	hqs	,354	21,218	9	,012	,711	,828	,250

Tests the null hypothesis that the error covariance matrix of the orthonormalized transformed dependent variables is proportional to an identity matrix.

a. May be used to adjust the degrees of freedom for the averaged tests of significance. Corrected tests are displayed in the Tests of Within-Subjects Effects table.
b. Design: Intercept
Within Subjects Design: interface

Univariate Tests

Source	Measure		Type III Sum of Squares	df	Mean Square	F	Sig.	Partial Eta Squared	Noncent. Parameter	Observed Power[a]
interface	pq	Sphericity Assumed	2,458	4	,614	4,052	,005	,156	16,206	,899
		Greenhouse-Geisser	2,458	2,885	,852	4,052	,012	,156	11,689	,809
		Huynh-Feldt	2,458	3,367	,730	4,052	,008	,156	13,641	,855
		Lower-bound	2,458	1,000	2,458	4,052	,057	,156	4,052	,486
	hqs	Sphericity Assumed	48,727	4	12,182	58,260	,000	,726	233,040	1,000
		Greenhouse-Geisser	48,727	2,844	17,131	58,260	,000	,726	165,711	1,000
		Huynh-Feldt	48,727	3,311	14,718	58,260	,000	,726	192,885	1,000
		Lower-bound	48,727	1,000	48,727	58,260	,000	,726	58,260	1,000
Error(interface)	pq	Sphericity Assumed	13,346	88	,152					
		Greenhouse-Geisser	13,346	63,471	,210					
		Huynh-Feldt	13,346	74,070	,180					
		Lower-bound	13,346	22,000	,607					
	hqs	Sphericity Assumed	18,400	88	,209					
		Greenhouse-Geisser	18,400	62,575	,294					
		Huynh-Feldt	18,400	72,837	,253					
		Lower-bound	18,400	22,000	,836					

a. Computed using alpha = ,05

The p-values in the following table are not Bonferroni corrected. Bonferroni corrected values are p-value*0.1.

Pairwise Comparisons

Measure	(I) interface	(J) interface	Mean Difference (I-J)	Std. Error	Sig.[a]	95% Confidence Interval for Difference[a]	
						Lower Bound	Upper Bound
pq	1	2	,286	,096	,071	-,015	,586
		3	,056	,126	1,000	-,336	,448
		4	,267	,145	,799	-,187	,721
		5	,385	,135	,095	-,037	,808
	2	1	-,286	,096	,071	-,586	,015
		3	-,230	,110	,476	-,571	,112
		4	-,019	,117	1,000	-,383	,346
		5	,099	,112	1,000	-,249	,447
	3	1	-,056	,126	1,000	-,448	,336
		2	,230	,110	,476	-,112	,571
		4	,211	,118	,884	-,158	,581
		5	,329*	,093	,018	,040	,618
	4	1	-,267	,145	,799	-,721	,187
		2	,019	,117	1,000	-,346	,383
		3	-,211	,118	,884	-,581	,158
		5	,118	,081	1,000	-,135	,371
	5	1	-,385	,135	,095	-,808	,037
		2	-,099	,112	1,000	-,447	,249
		3	-,329*	,093	,018	-,618	-,040
		4	-,118	,081	1,000	-,371	,135
hqs	1	2	-,329*	,090	,014	-,611	-,047
		3	-1,199*	,165	,000	-1,714	-,684
		4	-1,621*	,132	,000	-2,031	-1,211
		5	-1,516*	,122	,000	-1,897	-1,134
	2	1	,329*	,090	,014	,047	,611
		3	-,870*	,146	,000	-1,325	-,414
		4	-1,292*	,132	,000	-1,705	-,879
		5	-1,186*	,139	,000	-1,619	-,754
	3	1	1,199*	,165	,000	,684	1,714
		2	,870*	,146	,000	,414	1,325
		4	-,422	,144	,078	-,873	,028
		5	-,317	,167	,708	-,837	,203
	4	1	1,621*	,132	,000	1,211	2,031
		2	1,292*	,132	,000	,879	1,705
		3	,422	,144	,078	-,028	,873
		5	,106	,085	1,000	-,160	,372
	5	1	1,516*	,122	,000	1,134	1,897
		2	1,186*	,139	,000	,754	1,619
		3	,317	,167	,708	-,203	,837
		4	-,106	,085	1,000	-,372	,160

Based on estimated marginal means

a. Adjustment for multiple comparisons: Bonferroni.
*. The mean difference is significant at the ,05 level.

A.2.3.3 Preference

Ranks

	Mean Rank
PrefMapHHD	2,11
PrefMapSW	4,11
PrefMapHMD	2,89
PrefMapSWRef	3,11
PrefMapBodyRef	2,78

Test Statistics[a]

N	23
Chi-Square	19,354
df	4
Asymp. Sig.	,001

a. Friedman Test

The p-values in the following table are not Bonferroni corrected. Bonferroni corrected values are p-value*0.1

Test Statistics[c]

	PrefMapSW - PrefMapHHD	PrefMapHMD - PrefMapHHD	PrefMap SWRef - PrefMapHHD	PrefMapBody Ref - PrefMapHHD	PrefMapHMD - PrefMapSW	PrefMap SWRef - PrefMapSW	PrefMapBody Ref - PrefMapSW	PrefMap SWRef - PrefMapHMD	PrefMapBody Ref - PrefMapHMD	PrefMap SWRef - PrefMapBody Ref
Z	-4,250[a]	-1,762[a]	-2,235[a]	-1,200[a]	-2,537[b]	-2,146[b]	-2,273[b]	-,386[a]	-,140[b]	-,664[a]
Asymp. Sig. (2-tailed)	,000	,078	,025	,230	,011	,032	,023	,700	,889	,507

a. Based on negative ranks.
b. Based on positive ranks.
c. Wilcoxon Signed Ranks Test

A.3 Detailed Statistics for Experiment 2: 1D Target Acquisition

A.3.1 Task Completion Time

IF: interface, dir: direction

A.3.1.1 Descriptive Statistics

Estimates

Measure:TCT

IF	Mean	Std. Error	95% Confidence Interval	
			Lower Bound	Upper Bound
1	2,363	,027	2,310	2,416
2	3,952	,046	3,861	4,043
3	3,971	,053	3,866	4,075
4	2,938	,053	2,833	3,042
5	3,778	,066	3,648	3,907

7. dir * length

Measure:TCT

dir	length	Mean	Std. Error	95% Confidence Interval	
				Lower Bound	Upper Bound
1	1	2,569	,033	2,505	2,634
	2	4,248	,043	4,163	4,333
2	1	2,530	,028	2,474	2,585
	2	4,254	,065	4,126	4,381

Estimates

Measure:TCT

dir	Mean	Std. Error	95% Confidence Interval	
			Lower Bound	Upper Bound
1	3,409	,034	3,342	3,475
2	3,392	,042	3,309	3,474

Estimates

Measure:TCT

length	Mean	Std. Error	95% Confidence Interval	
			Lower Bound	Upper Bound
1	2,549	,027	2,497	2,602
2	4,251	,047	4,158	4,344

5. IF * dir

Measure:TCT

IF	dir	Mean	Std. Error	95% Confidence Interval	
				Lower Bound	Upper Bound
1	1	2,338	,031	2,278	2,399
	2	2,388	,030	2,329	2,447
2	1	3,995	,043	3,910	4,079
	2	3,909	,067	3,777	4,042
3	1	4,087	,058	3,972	4,202
	2	3,854	,063	3,729	3,979
4	1	2,844	,057	2,730	2,957
	2	3,031	,071	2,891	3,172
5	1	3,780	,064	3,653	3,907
	2	3,775	,093	3,592	3,958

6. IF * length

Measure:TCT

IF	length	Mean	Std. Error	95% Confidence Interval	
				Lower Bound	Upper Bound
1	1	1,798	,025	1,749	1,847
	2	2,928	,036	2,856	3,000
2	1	2,838	,028	2,783	2,894
	2	5,066	,074	4,920	5,211
3	1	2,884	,043	2,800	2,969
	2	5,057	,073	4,913	5,201
4	1	2,451	,059	2,335	2,566
	2	3,424	,068	3,290	3,559
5	1	2,776	,048	2,681	2,871
	2	4,779	,104	4,575	4,984

8. IF * dir * length

Measure:TCT

IF	dir	length	Mean	Std. Error	95% Confidence Interval	
					Lower Bound	Upper Bound
1	1	1	1,764	,033	1,699	1,829
		2	2,912	,041	2,831	2,994
	2	1	1,832	,029	1,776	1,889
		2	2,944	,041	2,863	3,025
2	1	1	2,880	,035	2,810	2,950
		2	5,109	,061	4,989	5,230
	2	1	2,797	,032	2,733	2,861
		2	5,022	,120	4,786	5,258
3	1	1	2,940	,055	2,830	3,049
		2	5,235	,082	5,074	5,396
	2	1	2,829	,053	2,724	2,935
		2	4,879	,089	4,703	5,055
4	1	1	2,358	,065	2,230	2,487
		2	3,329	,081	3,170	3,489
	2	1	2,544	,081	2,384	2,703
		2	3,519	,094	3,333	3,705
5	1	1	2,906	,085	2,737	3,074
		2	4,654	,074	4,508	4,801
	2	1	2,646	,034	2,578	2,713
		2	4,904	,175	4,559	5,250

A.3.1.2 Analysis of Variance

Mauchly's Test of Sphericity[b]

Measure:TCT

Within Subjects Effect	Mauchly's W	Approx. Chi-Square	df	Sig.	Epsilon[a]		
					Greenhouse-Geisser	Huynh-Feldt	Lower-bound
IF	,591	95,513	9	,000	,829	,846	,250
dir	1,000	,000	0	.	1,000	1,000	1,000
length	1,000	,000	0	.	1,000	1,000	1,000
IF * dir	,595	94,178	9	,000	,819	,835	,250
IF * length	,550	108,294	9	,000	,809	,825	,250
dir * length	1,000	,000	0	.	1,000	1,000	1,000
IF * dir * length	,402	165,451	9	,000	,709	,721	,250

Tests the null hypothesis that the error covariance matrix of the orthonormalized transformed dependent variables is proportional to an identity matrix.

a. May be used to adjust the degrees of freedom for the averaged tests of significance. Corrected tests are displayed in the Tests of Within-Subjects Effects table.
b. Design: Intercept
Within Subjects Design: IF + dir + length + IF * dir + IF * length + dir * length + IF * dir * length

Tests of Within-Subjects Effects

Measure:TCT

Source		Type III Sum of Squares	df	Mean Square	F	Sig.	Partial Eta Squared	Noncent. Parameter	Observed Power[a]
IF	Sphericity Assumed	1517,230	4	379,308	301,017	,000	,622	1204,066	1,000
	Greenhouse-Geisser	1517,230	3,315	457,699	301,017	,000	,622	997,842	1,000
	Huynh-Feldt	1517,230	3,383	448,436	301,017	,000	,622	1018,454	1,000
	Lower-bound	1517,230	1,000	1517,230	301,017	,000	,622	301,017	1,000
Error(IF)	Sphericity Assumed	922,385	732	1,260					
	Greenhouse-Geisser	922,385	606,628	1,521					
	Huynh-Feldt	922,385	619,159	1,490					
	Lower-bound	922,385	183,000	5,040					
dir	Sphericity Assumed	,270	1	,270	,284	,595	,002	,284	,083
	Greenhouse-Geisser	,270	1,000	,270	,284	,595	,002	,284	,083
	Huynh-Feldt	,270	1,000	,270	,284	,595	,002	,284	,083
	Lower-bound	,270	1,000	,270	,284	,595	,002	,284	,083
Error(dir)	Sphericity Assumed	174,084	183	,951					
	Greenhouse-Geisser	174,084	183,000	,951					
	Huynh-Feldt	174,084	183,000	,951					
	Lower-bound	174,084	183,000	,951					
length	Sphericity Assumed	2663,011	1	2663,011	2547,226	,000	,933	2547,226	1,000
	Greenhouse-Geisser	2663,011	1,000	2663,011	2547,226	,000	,933	2547,226	1,000
	Huynh-Feldt	2663,011	1,000	2663,011	2547,226	,000	,933	2547,226	1,000
	Lower-bound	2663,011	1,000	2663,011	2547,226	,000	,933	2547,226	1,000
Error(length)	Sphericity Assumed	191,318	183	1,045					
	Greenhouse-Geisser	191,318	183,000	1,045					
	Huynh-Feldt	191,318	183,000	1,045					
	Lower-bound	191,318	183,000	1,045					
IF * dir	Sphericity Assumed	18,009	4	4,502	5,712	,000	,030	22,848	,981
	Greenhouse-Geisser	18,009	3,274	5,500	5,712	,000	,030	18,701	,961
	Huynh-Feldt	18,009	3,341	5,391	5,712	,000	,030	19,082	,963
	Lower-bound	18,009	1,000	18,009	5,712	,018	,030	5,712	,662
Error(IF*dir)	Sphericity Assumed	576,964	732	,788					
	Greenhouse-Geisser	576,964	599,149	,963					
	Huynh-Feldt	576,964	611,361	,944					
	Lower-bound	576,964	183,000	3,153					
IF * length	Sphericity Assumed	266,151	4	66,538	89,486	,000	,328	357,945	1,000
	Greenhouse-Geisser	266,151	3,236	82,240	89,486	,000	,328	289,600	1,000
	Huynh-Feldt	266,151	3,301	80,618	89,486	,000	,328	295,429	1,000
	Lower-bound	266,151	1,000	266,151	89,486	,000	,328	89,486	1,000
Error(IF*length)	Sphericity Assumed	544,280	732	,744					
	Greenhouse-Geisser	544,280	592,235	,919					
	Huynh-Feldt	544,280	604,155	,901					
	Lower-bound	544,280	183,000	2,974					
dir * length	Sphericity Assumed	,477	1	,477	,532	,467	,003	,532	,112
	Greenhouse-Geisser	,477	1,000	,477	,532	,467	,003	,532	,112
	Huynh-Feldt	,477	1,000	,477	,532	,467	,003	,532	,112
	Lower-bound	,477	1,000	,477	,532	,467	,003	,532	,112
Error(dir*length)	Sphericity Assumed	164,140	183	,897					
	Greenhouse-Geisser	164,140	183,000	,897					
	Huynh-Feldt	164,140	183,000	,897					
	Lower-bound	164,140	183,000	,897					
IF * dir * length	Sphericity Assumed	14,329	4	3,582	4,582	,001	,024	18,327	,946
	Greenhouse-Geisser	14,329	2,835	5,055	4,582	,004	,024	12,988	,874
	Huynh-Feldt	14,329	2,884	4,969	4,582	,004	,024	13,213	,878
	Lower-bound	14,329	1,000	14,329	4,582	,034	,024	4,582	,567
Error(IF*dir*length)	Sphericity Assumed	572,315	732	,782					
	Greenhouse-Geisser	572,315	518,733	1,103					
	Huynh-Feldt	572,315	527,742	1,084					
	Lower-bound	572,315	183,000	3,127					

a. Computed using alpha = ,05

A.3.1.3 Simple Main Effects

Pairwise Comparisons

Measure:TCT

(I) IF	(J) IF	Mean Difference (I-J)	Std. Error	Sig.[a]	95% Confidence Interval for Difference[a]	
					Lower Bound	Upper Bound
1	2	-1,589*	,039	,000	-1,699	-1,478
	3	-1,607*	,046	,000	-1,737	-1,477
	4	-,574*	,052	,000	-,723	-,426
	5	-1,414*	,061	,000	-1,587	-1,242
2	1	1,589*	,039	,000	1,478	1,699
	3	-,019	,052	1,000	-,167	,129
	4	1,014*	,059	,000	,846	1,182
	5	,174	,064	,073	-,008	,357
3	1	1,607*	,046	,000	1,477	1,737
	2	,019	,052	1,000	-,129	,167
	4	1,033*	,067	,000	,844	1,222
	5	,193	,068	,052	-,001	,387
4	1	,574*	,052	,000	,426	,723
	2	-1,014*	,059	,000	-1,182	-,846
	3	-1,033*	,067	,000	-1,222	-,844
	5	-,840*	,069	,000	-1,036	-,644
5	1	1,414*	,061	,000	1,242	1,587
	2	-,174	,064	,073	-,357	,008
	3	-,193	,068	,052	-,387	,001
	4	,840*	,069	,000	,644	1,036

Based on estimated marginal means

*. The mean difference is significant at the ,05 level.
a. Adjustment for multiple comparisons: Bonferroni.

Pairwise Comparisons

Measure:TCT

(I) dir	(J) dir	Mean Difference (I-J)	Std. Error	Sig.[a]	95% Confidence Interval for Difference[a]	
					Lower Bound	Upper Bound
1	2	,017	,032	,595	-,046	,081
2	1	-,017	,032	,595	-,081	,046

Based on estimated marginal means

a. Adjustment for multiple comparisons: Bonferroni.

Pairwise Comparisons

Measure:TCT

(I) length	(J) length	Mean Difference (I-J)	Std. Error	Sig.[a]	95% Confidence Interval for Difference[a]	
					Lower Bound	Upper Bound
1	2	-1,701*	,034	,000	-1,768	-1,635
2	1	1,701*	,034	,000	1,635	1,768

Based on estimated marginal means

*. The mean difference is significant at the ,05 level.
a. Adjustment for multiple comparisons: Bonferroni.

A.3.1.4 Two-Way Interactions

IFDirSS: Interface * Direction (direction fixed at level: same side of smartwatch)

Mauchly's Test of Sphericity[b]

Measure:TCT

Within Subjects Effect	Mauchly's W	Approx. Chi-Square	df	Sig.	Epsilon[a]		
					Greenhouse-Geisser	Huynh-Feldt	Lower-bound
IFDirSS	,622	173,245	9	,000	,818	,826	,250

Tests the null hypothesis that the error covariance matrix of the orthonormalized transformed dependent variables is proportional to an identity matrix.

a. May be used to adjust the degrees of freedom for the averaged tests of significance. Corrected tests are displayed in the Tests of Within-Subjects Effects table.
b. Design: Intercept
Within Subjects Design: IFDirSS

Tests of Within-Subjects Effects

Measure:TCT

Source		Type III Sum of Squares	df	Mean Square	F	Sig.	Partial Eta Squared	Noncent. Parameter	Observed Power[a]
IFDirSS	Sphericity Assumed	885,533	4	221,383	316,348	,000	,463	1265,392	1,000
	Greenhouse-Geisser	885,533	3,273	270,588	316,348	,000	,463	1035,288	1,000
	Huynh-Feldt	885,533	3,306	267,891	316,348	,000	,463	1045,710	1,000
	Lower-bound	885,533	1,000	885,533	316,348	,000	,463	316,348	1,000
Error(IFDirSS)	Sphericity Assumed	1027,321	1468	,700					
	Greenhouse-Geisser	1027,321	1201,053	,855					
	Huynh-Feldt	1027,321	1213,144	,847					
	Lower-bound	1027,321	367,000	2,799					

a. Computed using alpha = ,05

Pairwise Comparisons

Measure:TCT

(I) IFDirSS	(J) IFDirSS	Mean Difference (I-J)	Std. Error	Sig.[a]	95% Confidence Interval for Difference[a]	
					Lower Bound	Upper Bound
1	2	-1,656*	,046	,000	-1,788	-1,525
	3	-1,749*	,058	,000	-1,913	-1,585
	4	-,505*	,056	,000	-,663	-,348
	5	-1,442*	,060	,000	-1,611	-1,272
2	1	1,656*	,046	,000	1,525	1,788
	3	-,093	,049	,575	-,230	,045
	4	1,151*	,067	,000	,961	1,341
	5	,215*	,058	,003	,050	,379
3	1	1,749*	,058	,000	1,585	1,913
	2	,093	,049	,575	-,045	,230
	4	1,243*	,076	,000	1,030	1,457
	5	,307*	,066	,000	,121	,493
4	1	,505*	,056	,000	,348	,663
	2	-1,151*	,067	,000	-1,341	-,961
	3	-1,243*	,076	,000	-1,457	-1,030
	5	-,936*	,074	,000	-1,145	-,728
5	1	1,442*	,060	,000	1,272	1,611
	2	-,215*	,058	,003	-,379	-,050
	3	-,307*	,066	,000	-,493	-,121
	4	,936*	,074	,000	,728	1,145

Based on estimated marginal means

*. The mean difference is significant at the ,05 level.
a. Adjustment for multiple comparisons: Bonferroni.

IFDirSO: Interface * Direction (direction fixed at level: opposite side of smartwatch arm)

Mauchly's Test of Sphericity[b]

Measure:TCT

Within Subjects Effect	Mauchly's W	Approx. Chi-Square	df	Sig.	Epsilon[a]		
					Greenhouse-Geisser	Huynh-Feldt	Lower-bound
IFDirSO	,490	260,345	9	,000	,780	,788	,250

Tests the null hypothesis that the error covariance matrix of the orthonormalized transformed dependent variables is proportional to an identity matrix.

a. May be used to adjust the degrees of freedom for the averaged tests of significance. Corrected tests are displayed in the Tests of Within-Subjects Effects table.
b. Design: Intercept
Within Subjects Design: IFDirSO

Tests of Within-Subjects Effects

Measure:TCT

Source		Type III Sum of Squares	df	Mean Square	F	Sig.	Partial Eta Squared	Noncent. Parameter	Observed Power[a]
IFDirSO	Sphericity Assumed	649,705	4	162,426	127,570	,000	,258	510,281	1,000
	Greenhouse-Geisser	649,705	3,121	208,174	127,570	,000	,258	398,143	1,000
	Huynh-Feldt	649,705	3,151	206,202	127,570	,000	,258	401,951	1,000
	Lower-bound	649,705	1,000	649,705	127,570	,000	,258	127,570	1,000
Error(IFDirSO)	Sphericity Assumed	1869,103	1468	1,273					
	Greenhouse-Geisser	1869,103	1145,397	1,632					
	Huynh-Feldt	1869,103	1156,352	1,616					
	Lower-bound	1869,103	367,000	5,093					

a. Computed using alpha = ,05

Pairwise Comparisons

Measure:TCT

(I) IFDirSO	(J) IFDirSO	Mean Difference (I-J)	Std. Error	Sig.[a]	95% Confidence Interval for Difference[a]	
					Lower Bound	Upper Bound
1	2	-1,521*	,066	,000	-1,709	-1,333
	3	-1,466*	,055	,000	-1,621	-1,310
	4	-,643*	,062	,000	-,819	-,467
	5	-1,387*	,093	,000	-1,648	-1,125
2	1	1,521*	,066	,000	1,333	1,709
	3	,055	,072	1,000	-,149	,260
	4	,878*	,089	,000	,627	1,129
	5	,134	,102	1,000	-,153	,422
3	1	1,466*	,055	,000	1,310	1,621
	2	-,055	,072	1,000	-,260	,149
	4	,823*	,083	,000	,588	1,057
	5	,079	,097	1,000	-,194	,352
4	1	,643*	,062	,000	,467	,819
	2	-,878*	,089	,000	-1,129	-,627
	3	-,823*	,083	,000	-1,057	-,588
	5	-,744*	,098	,000	-1,020	-,468
5	1	1,387*	,093	,000	1,125	1,648
	2	-,134	,102	1,000	-,422	,153
	3	-,079	,097	1,000	-,352	,194
	4	,744*	,098	,000	,468	1,020

Based on estimated marginal means

*. The mean difference is significant at the ,05 level.
a. Adjustment for multiple comparisons: Bonferroni.

IFLengthShort: Interface * Length (length fixed at level: short)

Mauchly's Test of Sphericity[b]

Measure:TCT

Within Subjects Effect	Mauchly's W	Approx. Chi-Square	df	Sig.	Epsilon[a]		
					Greenhouse-Geisser	Huynh-Feldt	Lower-bound
IFLengthShort	,452	290,069	9	,000	,765	,772	,250

Tests the null hypothesis that the error covariance matrix of the orthonormalized transformed dependent variables is proportional to an identity matrix.

a. May be used to adjust the degrees of freedom for the averaged tests of significance. Corrected tests are displayed in the Tests of Within-Subjects Effects table.
b. Design: Intercept
Within Subjects Design: IFLengthShort

Tests of Within-Subjects Effects

Measure:TCT

Source		Type III Sum of Squares	df	Mean Square	F	Sig.	Partial Eta Squared	Noncent. Parameter	Observed Power[a]
IFLengthShort	Sphericity Assumed	302,054	4	75,513	162,097	,000	,306	648,389	1,000
	Greenhouse-Geisser	302,054	3,059	98,736	162,097	,000	,306	495,887	1,000
	Huynh-Feldt	302,054	3,088	97,821	162,097	,000	,306	500,527	1,000
	Lower-bound	302,054	1,000	302,054	162,097	,000	,306	162,097	1,000
Error(IFLengthShort)	Sphericity Assumed	683,872	1468	,466					
	Greenhouse-Geisser	683,872	1122,723	,609					
	Huynh-Feldt	683,872	1133,229	,603					
	Lower-bound	683,872	367,000	1,863					

a. Computed using alpha = ,05

Pairwise Comparisons

Measure:TCT

(I) IFLengthShort	(J) IFLengthShort	Mean Difference (I-J)	Std. Error	Sig.[a]	95% Confidence Interval for Difference[a]	
					Lower Bound	Upper Bound
1	2	-1,040*	,028	,000	-1,119	-,962
	3	-1,086*	,039	,000	-1,197	-,975
	4	-,653*	,052	,000	-,801	-,504
	5	-,977*	,050	,000	-1,117	-,838
2	1	1,040*	,028	,000	,962	1,119
	3	-,046	,039	1,000	-,156	,065
	4	,387*	,054	,000	,236	,539
	5	,063	,049	1,000	-,074	,200
3	1	1,086*	,039	,000	,975	1,197
	2	,046	,039	1,000	-,065	,156
	4	,433*	,060	,000	,264	,603
	5	,109	,056	,536	-,050	,267
4	1	,653*	,052	,000	,504	,801
	2	-,387*	,054	,000	-,539	-,236
	3	-,433*	,060	,000	-,603	-,264
	5	-,325*	,065	,000	-,509	-,140
5	1	,977*	,050	,000	,838	1,117
	2	-,063	,049	1,000	-,200	,074
	3	-,109	,056	,536	-,267	,050
	4	,325*	,065	,000	,140	,509

Based on estimated marginal means

*. The mean difference is significant at the ,05 level.
a. Adjustment for multiple comparisons: Bonferroni.

IFLengthLong: Interface * Length (length fixed at level: long)

Mauchly's Test of Sphericity[b]

Measure:TCT

Within Subjects Effect	Mauchly's W	Approx. Chi-Square	df	Sig.	Epsilon[a]		
					Greenhouse-Geisser	Huynh-Feldt	Lower-bound
IFLengthLong	,517	240,904	9	,000	,782	,789	,250

Tests the null hypothesis that the error covariance matrix of the orthonormalized transformed dependent variables is proportional to an identity matrix.

a. May be used to adjust the degrees of freedom for the averaged tests of significance. Corrected tests are displayed in the Tests of Within-Subjects Effects table.
b. Design: Intercept
Within Subjects Design: IFLengthLong

Tests of Within-Subjects Effects

Measure:TCT

Source		Type III Sum of Squares	df	Mean Square	F	Sig.	Partial Eta Squared	Noncent. Parameter	Observed Power[a]
IFLengthLong	Sphericity Assumed	1481,327	4	370,332	276,748	,000	,430	1106,992	1,000
	Greenhouse-Geisser	1481,327	3,128	473,642	276,748	,000	,430	865,536	1,000
	Huynh-Feldt	1481,327	3,158	469,145	276,748	,000	,430	873,833	1,000
	Lower-bound	1481,327	1,000	1481,327	276,748	,000	,430	276,748	1,000
Error(IFLengthLong)	Sphericity Assumed	1964,411	1468	1,338					
	Greenhouse-Geisser	1964,411	1147,801	1,711					
	Huynh-Feldt	1964,411	1158,803	1,695					
	Lower-bound	1964,411	367,000	5,353					

a. Computed using alpha = ,05

Pairwise Comparisons

Measure:TCT

(I) IFLengthLong	(J) IFLengthLong	Mean Difference (I-J)	Std. Error	Sig.[a]	95% Confidence Interval for Difference[a]	
					Lower Bound	Upper Bound
1	2	-2,137*	,065	,000	-2,320	-1,954
	3	-2,129*	,059	,000	-2,295	-1,962
	4	-,496*	,065	,000	-,680	-,312
	5	-1,851*	,093	,000	-2,114	-1,588
2	1	2,137*	,065	,000	1,954	2,320
	3	,009	,078	1,000	-,212	,229
	4	1,641*	,087	,000	1,396	1,886
	5	,286	,107	,075	-,015	,587
3	1	2,129*	,059	,000	1,962	2,295
	2	-,009	,078	1,000	-,229	,212
	4	1,633*	,085	,000	1,391	1,874
	5	,277	,103	,072	-,012	,567
4	1	,496*	,065	,000	,312	,680
	2	-1,641*	,087	,000	-1,886	-1,396
	3	-1,633*	,085	,000	-1,874	-1,391
	5	-1,355*	,097	,000	-1,628	-1,082
5	1	1,851*	,093	,000	1,588	2,114
	2	-,286	,107	,075	-,587	,015
	3	-,277	,103	,072	-,567	,012
	4	1,355*	,097	,000	1,082	1,628

Based on estimated marginal means

*. The mean difference is significant at the ,05 level.
a. Adjustment for multiple comparisons: Bonferroni.

A.3.2 Errors

A.3.2.1 Effect of Interface

Ranks

	Mean Rank
HHD	2,87
SW	2,81
HMD	3,21
BodyRef	3,28
SWRef	2,82

Test Statistics[a]

N	740
Chi-Square	231,677
df	4
Asymp. Sig.	,000

a. Friedman Test

The p-values in the following table are not Bonferroni corrected. Bonferroni corrected values are p-value*0.1.

Test Statistics[c]

	SW - HHD	HMD - HHD	BodyRef - HHD	SWRef - HHD	HMD - SW	BodyRef - SW	SWRef - SW	BodyRef - HMD	SWRef - HMD	SWRef - BodyRef
Z	-1,973[a]	-7,582[b]	-8,753[b]	-1,637[a]	-8,885[b]	-9,777[b]	-,337[b]	-1,652[b]	-8,624[a]	-9,606[a]
Asymp. Sig. (2-tailed)	,049	,000	,000	,102	,000	,000	,736	,099	,000	,000

a. Based on positive ranks.
b. Based on negative ranks.
c. Wilcoxon Signed Ranks Test

A.3.2.2 Effect of Direction and Length

SWOSide: opposite side of smartwatch arm

SWSide: same side as smartwatch arm

Test Statistics[b]

	Long - Short	SWOSide - SWSide
Z	-,466[a]	-1,365[a]
Asymp. Sig. (2-tailed)	,641	,172

a. Based on negative ranks.
b. Wilcoxon Signed Ranks Test

A.3.3 Subjective Workload

interfaces: 1: HHD, 2: SW, 3: HMD, 4: BodyRef, 5: SWRef

md: mental demand, pd: physical demand, td: temporal demand, p: performance, e: effort, f: frustration, o: overall.

Mauchly's Test of Sphericity[b]

Within Subjects Effect	Measure	Mauchly's W	Approx. Chi-Square	df	Sig.	Epsilon[a]		
						Greenhouse-Geisser	Huynh-Feldt	Lower-bound
Interface	md	,156	36,024	9	,000	,655	,757	,250
	pd	,364	19,625	9	,021	,723	,850	,250
	td	,390	18,283	9	,033	,718	,844	,250
	p	,462	14,974	9	,093	,756	,897	,250
	e	,166	34,878	9	,000	,617	,705	,250
	f	,779	4,856	9	,847	,910	1,000	,250
	o	,551	11,588	9	,239	,798	,957	,250

Tests the null hypothesis that the error covariance matrix of the orthonormalized transformed dependent variables is proportional to an identity matrix.

a. May be used to adjust the degrees of freedom for the averaged tests of significance. Corrected tests are displayed in the Tests of Within-Subjects Effects table.
b. Design: Intercept
Within Subjects Design: Interface

Univariate Tests

Source	Measure		Type III Sum of Squares	df	Mean Square	F	Sig.	Partial Eta Squared	Noncent. Parameter	Observed Power[a]
Interface	md	Sphericity Assumed	3328,636	4	832,159	7,978	,000	,275	31,913	,997
		Greenhouse-Geisser	3328,636	2,620	1270,627	7,978	,000	,275	20,901	,977
		Huynh-Feldt	3328,636	3,027	1099,733	7,978	,000	,275	24,149	,987
		Lower-bound	3328,636	1,000	3328,636	7,978	,010	,275	7,978	,768
	pd	Sphericity Assumed	8850,909	4	2212,727	8,658	,000	,292	34,630	,999
		Greenhouse-Geisser	8850,909	2,891	3061,878	8,658	,000	,292	25,026	,990
		Huynh-Feldt	8850,909	3,401	2602,226	8,658	,000	,292	29,447	,996
		Lower-bound	8850,909	1,000	8850,909	8,658	,008	,292	8,658	,801
	td	Sphericity Assumed	1435,000	4	358,750	1,852	,127	,081	7,406	,540
		Greenhouse-Geisser	1435,000	2,873	499,464	1,852	,150	,081	5,320	,447
		Huynh-Feldt	1435,000	3,377	424,981	1,852	,139	,081	6,252	,490
		Lower-bound	1435,000	1,000	1435,000	1,852	,188	,081	1,852	,255
	p	Sphericity Assumed	1024,091	4	256,023	1,889	,120	,083	7,555	,550
		Greenhouse-Geisser	1024,091	3,023	338,758	1,889	,140	,083	5,710	,469
		Huynh-Feldt	1024,091	3,588	285,392	1,889	,128	,083	6,778	,517
		Lower-bound	1024,091	1,000	1024,091	1,889	,184	,083	1,889	,259
	e	Sphericity Assumed	5867,273	4	1466,818	6,754	,000	,243	27,016	,991
		Greenhouse-Geisser	5867,273	2,467	2378,273	6,754	,001	,243	16,663	,940
		Huynh-Feldt	5867,273	2,821	2080,128	6,754	,001	,243	19,051	,961
		Lower-bound	5867,273	1,000	5867,273	6,754	,017	,243	6,754	,698
	f	Sphericity Assumed	4266,818	4	1066,705	5,613	,000	,211	22,452	,973
		Greenhouse-Geisser	4266,818	3,642	1171,677	5,613	,001	,211	20,441	,962
		Huynh-Feldt	4266,818	4,000	1066,705	5,613	,000	,211	22,452	,973
		Lower-bound	4266,818	1,000	4266,818	5,613	,027	,211	5,613	,618
	o	Sphericity Assumed	2706,711	4	676,678	8,089	,000	,278	32,357	,998
		Greenhouse-Geisser	2706,711	3,191	848,357	8,089	,000	,278	25,809	,991
		Huynh-Feldt	2706,711	3,829	706,905	8,089	,000	,278	30,973	,997
		Lower-bound	2706,711	1,000	2706,711	8,089	,010	,278	8,089	,774
Error(Interface)	md	Sphericity Assumed	8761,364	84	104,302					
		Greenhouse-Geisser	8761,364	55,013	159,259					
		Huynh-Feldt	8761,364	63,562	137,839					
		Lower-bound	8761,364	21,000	417,208					
	pd	Sphericity Assumed	21469,091	84	255,584					
		Greenhouse-Geisser	21469,091	60,704	353,667					
		Huynh-Feldt	21469,091	71,427	300,574					
		Lower-bound	21469,091	21,000	1022,338					
	td	Sphericity Assumed	16275,000	84	193,750					
		Greenhouse-Geisser	16275,000	60,335	269,745					
		Huynh-Feldt	16275,000	70,909	229,519					
		Lower-bound	16275,000	21,000	775,000					
	p	Sphericity Assumed	11385,909	84	135,547					
		Greenhouse-Geisser	11385,909	63,485	179,349					
		Huynh-Feldt	11385,909	75,356	151,096					
		Lower-bound	11385,909	21,000	542,186					
	e	Sphericity Assumed	18242,727	84	217,175					
		Greenhouse-Geisser	18242,727	51,808	352,124					
		Huynh-Feldt	18242,727	59,233	307,981					
		Lower-bound	18242,727	21,000	868,701					
	f	Sphericity Assumed	15963,182	84	190,038					
		Greenhouse-Geisser	15963,182	76,474	208,739					
		Huynh-Feldt	15963,182	84,000	190,038					
		Lower-bound	15963,182	21,000	760,152					
	o	Sphericity Assumed	7026,822	84	83,653					
		Greenhouse-Geisser	7026,822	67,001	104,876					
		Huynh-Feldt	7026,822	80,408	87,389					
		Lower-bound	7026,822	21,000	334,611					

a. Computed using alpha = ,05

Pairwise Comparisons

Measure	(I) Interface	(J) Interface	Mean Difference (I-J)	Std. Error	Sig.[a]	95% Confidence Interval for Difference[a]	
						Lower Bound	Upper Bound
md	1	2	-2.727	1.174	.300	-6.407	.952
		3	-8.409*	2.241	.012	-15.434	-1.384
		4	-14.318*	3.653	.008	-25.771	-2.866
		5	-12.500*	3.718	.020	-24.159	-.842
	2	1	2.727	1.174	.300	-.952	6.407
		3	-5.682	2.262	.200	-12.775	1.411
		4	-11.591*	3.675	.011	-21.220	-1.949
		5	-9.773	3.379	.087	-20.365	.820
	3	1	8.409*	2.241	.012	1.384	15.434
		2	5.682	2.262	.200	-1.411	12.775
		4	-5.909	3.813	1.000	-17.239	5.419
		5	-4.091	3.251	1.000	-14.282	6.101
	4	1	14.318*	3.653	.008	2.866	25.771
		2	11.591*	3.675	.011	1.949	21.233
		3	5.909	3.813	1.000	-5.419	17.239
		5	1.818	3.412	1.000	-8.878	12.514
	5	1	12.500*	3.718	.020	.842	24.159
		2	9.773	3.379	.087	-.820	20.365
		3	4.091	3.251	1.000	-6.101	14.282
		4	-1.818	3.412	1.000	-12.514	8.878
pd	1	2	-7.045	3.902	.853	-19.278	5.187
		3	-8.182	3.898	.475	-20.398	4.002
		4	-25.000*	4.948	.001	-40.505	-9.495
		5	-19.091*	4.880	.005	-34.700	-3.481
	2	1	7.045	3.902	.853	-5.187	19.278
		3	-1.136	4.901	1.000	-16.502	14.229
		4	-17.955	6.169	.094	-37.296	1.387
		5	-12.045	4.985	.249	-27.676	3.585
	3	1	8.182	3.898	.475	-4.002	20.398
		2	1.136	4.901	1.000	-14.229	16.502
		4	-16.818*	4.807	.021	-31.890	-1.746
		5	-10.909*	2.954	.014	-20.171	-1.647
	4	1	25.000*	4.948	.001	9.495	40.505
		2	17.955	6.169	.094	-1.387	37.296
		3	16.818*	4.807	.021	1.746	31.890
		5	5.909	6.099	1.000	-13.180	25.001
	5	1	19.091*	4.880	.005	3.481	33.700
		2	12.045	4.985	.249	-3.585	27.676
		3	10.909*	2.954	.014	1.647	20.171
		4	-5.909	6.099	1.000	-25.001	13.180
id	1	2	-7.500	4.274	.938	-20.898	5.898
		3	-7.045	4.507	1.000	-21.175	7.084
		4	-10.682	3.939	.130	-23.028	1.665
		5	-8.636	5.006	1.000	-25.220	8.000
	2	1	7.500	4.274	.938	-5.898	20.898
		3	.455	3.905	1.000	-11.799	12.699
		4	-3.182	3.730	1.000	-14.876	8.512
		5	-1.136	4.499	1.000	-15.239	12.965
	3	1	7.045	4.507	1.000	-7.084	21.175
		2	-.455	3.905	1.000	-12.699	11.789
		4	-3.636	4.268	1.000	-17.012	9.739
		5	-1.591	2.381	1.000	-9.056	5.874
	4	1	10.682	3.939	.130	-1.665	23.028
		2	3.182	3.730	1.000	-8.512	14.876
		3	3.636	4.268	1.000	-9.739	17.012
		5	2.045	4.542	1.000	-12.196	16.287
	5	1	8.636	5.006	1.000	-8.000	25.270
		2	1.136	4.499	1.000	-12.965	15.238
		3	1.591	2.381	1.000	-5.874	9.056
		4	-2.045	4.542	1.000	-16.287	12.196
p	1	2	-5.909	2.271	.166	-13.029	1.210
		3	-6.136	3.998	1.000	-18.639	6.368
		4	-8.591	3.213	.329	-18.684	3.482
		5	-9.318*	2.874	.009	-18.327	-.309
	2	1	5.909	2.271	.166	-1.210	13.029
		3	-.227	4.190	1.000	-13.394	12.879
		4	-2.682	3.808	1.000	-14.594	10.231
		5	-3.409	2.359	1.000	-10.800	3.984
	3	1	6.136	3.998	1.000	-6.368	18.639
		2	.227	4.190	1.000	-12.879	13.334
		4	-2.455	4.237	1.000	-15.740	10.831
		5	-3.182	4.194	1.000	-16.332	9.968
	4	1	8.591	3.213	.329	-3.482	18.664
		2	2.682	3.808	1.000	-10.831	14.194
		3	2.455	4.237	1.000	-10.831	15.740
		5	-.727	3.462	1.000	-13.590	12.126
	5	1	9.318*	2.874	.009	.309	18.327
		2	3.409	2.359	1.000	-3.984	10.800
		3	3.182	4.194	1.000	-9.968	16.332
		4	2.727	3.462	1.000	-8.126	13.590
e	1	2	-5.455	2.301	.274	-12.869	1.959
		3	-6.364	3.000	.460	-15.770	3.043
		4	-20.455*	5.304	.010	-37.178	-3.731
		5	-15.000*	4.745	.047	-29.875	-.125
	2	1	5.455	2.301	.274	-1.959	12.869
		3	-.909	3.659	1.000	-12.378	10.559
		4	-15.000	5.602	.141	-32.564	2.564
		5	-9.545	4.945	.672	-25.049	5.957
	3	1	6.364	3.000	.460	-3.043	15.770
		2	.909	3.659	1.000	-10.559	12.378
		4	-14.091	5.442	.171	-31.152	2.971
		5	-8.636	3.124	.116	-18.431	1.159
	4	1	20.455*	5.304	.010	3.731	37.178
		2	15.000	5.602	.141	-2.564	32.564
		3	14.091	5.442	.171	-2.971	31.152
		5	5.455	4.858	1.000	-9.771	20.680
	5	1	15.000*	4.745	.047	.125	29.875
		2	9.545	4.945	.672	-5.957	25.049
		3	8.636	3.124	.116	-1.159	18.431
		4	-5.455	4.858	1.000	-20.680	9.771

Based on estimated marginal means

a. Adjustment for multiple comparisons: Bonferroni.
*. The mean difference is significant at the .05 level.

Pairwise Comparisons

Measure	(I) Interface	(J) Interface	Mean Difference (I-J)	Std. Error	Sig.[a]	95% Confidence Interval for Difference[a]	
						Lower Bound	Upper Bound
f	1	2	-14,773*	3,473	,004	-25,663	-3,883
		3	-3,409	3,898	1,000	-15,630	8,812
		4	-5,227	3,314	1,000	-15,617	5,163
		5	-15,455*	4,014	,009	-28,041	-2,868
	2	1	14,773*	3,473	,004	3,883	25,663
		3	11,364	4,489	,194	-2,710	25,437
		4	9,545	4,326	,386	-4,017	23,108
		5	-,682	4,113	1,000	-13,576	12,213
	3	1	3,409	3,898	1,000	-8,812	15,630
		2	-11,364	4,489	,194	-25,437	2,710
		4	-1,818	4,565	1,000	-16,130	12,494
		5	-12,045	4,763	,195	-26,980	2,889
	4	1	5,227	3,314	1,000	-5,163	15,617
		2	-9,545	4,326	,386	-23,108	4,017
		3	1,818	4,565	1,000	-12,494	16,130
		5	-10,227	4,370	,292	-23,929	3,474
	5	1	15,455*	4,014	,009	2,868	28,041
		2	,682	4,113	1,000	-12,213	13,576
		3	12,045	4,763	,195	-2,889	26,980
		4	10,227	4,370	,292	-3,474	23,929
o	1	2	-7,106*	2,041	,022	-13,506	-,706
		3	-6,894*	2,159	,044	-13,662	-,126
		4	-13,864*	2,796	,001	-22,629	-5,098
		5	-12,765*	3,284	,009	-23,062	-2,469
	2	1	7,106*	2,041	,022	,706	13,506
		3	,212	2,428	1,000	-7,400	7,824
		4	-6,758	2,755	,230	-15,395	1,880
		5	-5,659	2,951	,688	-14,910	3,592
	3	1	6,894*	2,159	,044	,126	13,662
		2	-,212	2,428	1,000	-7,824	7,400
		4	-6,970	2,946	,277	-16,208	2,268
		5	-5,871	2,470	,270	-13,615	1,872
	4	1	13,864*	2,796	,001	5,098	22,629
		2	6,758	2,755	,230	-1,880	15,395
		3	6,970	2,946	,277	-2,268	16,208
		5	1,098	3,413	1,000	-9,601	11,798
	5	1	12,765*	3,284	,009	2,469	23,062
		2	5,659	2,951	,688	-3,592	14,910
		3	5,871	2,470	,270	-1,872	13,615
		4	-1,098	3,413	1,000	-11,798	9,601

Based on estimated marginal means

a. Adjustment for multiple comparisons: Bonferroni.
*. The mean difference is significant at the ,05 level.

A.3.4 User Experience

A.3.4.1 After Scenario Questionnaire

C1: HHD, C2: SW, C3: HMD, C4: BodyRef, C5: SWRef

A.3.4.1.1 Ease of Use

Ranks

	Mean Rank
eC1	3,83
eC2	3,30
eC3	3,17
eC4	2,65
eC5	2,04

Test Statistics[a]

N	23
Chi-Square	24,815
df	4
Asymp. Sig.	,000

a. Friedman Test

The p-values in the following table are not Bonferroni corrected. Bonferroni corrected values are p-value*0.1.

Test Statistics[b]

	eC2 - eC1	eC3 - eC1	eC4 - eC1	eC5 - eC1	eC3 - eC2	eC4 - eC2	eC5 - eC2	eC4 - eC3	eC5 - eC3	eC5 - eC4
Z	-1,807[a]	-2,496[a]	-2,632[a]	-3,475[a]	-,263[a]	-1,412[a]	-2,630[a]	-1,313[a]	-2,979[a]	-,980[a]
Asymp. Sig. (2-tailed)	,071	,013	,008	,001	,793	,158	,009	,189	,003	,327

a. Based on positive ranks.
b. Wilcoxon Signed Ranks Test

A.3.4.1.2 Satisfaction with Task Completion Time

Ranks

	Mean Rank
tC1	3,78
tC2	2,74
tC3	3,00
tC4	2,74
tC5	2,74

Test Statistics[a]

N	23
Chi-Square	11,148
df	4
Asymp. Sig.	,025

a. Friedman Test

The p-values in the following table are not Bonferroni corrected. Bonferroni corrected values are p-value*0.1.

Test Statistics[c]

	tC2 - tC1	tC3 - tC1	tC4 - tC1	tC5 - tC1	tC3 - tC2	tC4 - tC2	tC5 - tC2	tC5 - tC3	tC5 - tC4	tC4 - tC3
Z	-2,694[a]	-2,066[a]	-2,351[a]	-2,673[a]	-1,469[b]	-,964[b]	-,182[b]	-1,591[a]	-,854[a]	-,893[a]
Asymp. Sig. (2-tailed)	,007	,039	,019	,008	,142	,335	,856	,112	,393	,372

a. Based on positive ranks.
b. Based on negative ranks.
c. Wilcoxon Signed Ranks Test

A.3.4.1.3 Satisfaction with System Support

Ranks

	Mean Rank
sC1	3,96
sC2	2,37
sC3	3,54
sC4	2,83
sC5	2,30

Test Statistics[a]

N	23
Chi-Square	24,270
df	4
Asymp. Sig.	,000

a. Friedman Test

The p-values in the following table are not Bonferroni corrected. Bonferroni corrected values are p-value*0.1.

Test Statistics[c]

	sC2 - sC1	sC3 - sC1	sC4 - sC1	sC5 - sC1	sC3 - sC2	sC4 - sC2	sC5 - sC2	sC4 - sC3	sC5 - sC3	sC5 - sC4
Z	-3,036[a]	-1,284[a]	-2,230[a]	-3,237[a]	-2,477[b]	-1,059[b]	-,351[a]	-1,575[a]	-3,206[a]	-1,229[a]
Asymp. Sig. (2-tailed)	,002	,199	,026	,001	,013	,289	,726	,115	,001	,219

a. Based on positive ranks.
b. Based on negative ranks.
c. Wilcoxon Signed Ranks Test

A.3.4.2 Pragmatic Quality (PQ) and Hedonic Quality Stimulation (HQS)

interfaces: 1: HHD, 2: SW, 3: HMD, 4: BodyRef, 5: SWRef

Mauchly's Test of Sphericity[b]

Within Subjects Effect	Measure	Mauchly's W	Approx. Chi-Square	df	Sig.	Epsilon[a]		
						Greenhouse-Geisser	Huynh-Feldt	Lower-bound
interface	PQ	,336	22,271	9	,008	,690	,798	,250
	HQS	,553	12,110	9	,209	,803	,957	,250

Tests the null hypothesis that the error covariance matrix of the orthonormalized transformed dependent variables is proportional to an identity matrix.

a. May be used to adjust the degrees of freedom for the averaged tests of significance. Corrected tests are displayed in the Tests of Within-Subjects Effects table.
b. Design: Intercept
Within Subjects Design: interface

Univariate Tests

Source	Measure		Type III Sum of Squares	df	Mean Square	F	Sig.	Partial Eta Squared	Noncent. Parameter	Observed Power[a]
interface	PQ	Sphericity Assumed	3,149	4	,787	5,792	,000	,208	23,170	,977
		Greenhouse-Geisser	3,149	2,759	1,142	5,792	,002	,208	15,980	,924
		Huynh-Feldt	3,149	3,194	,986	5,792	,001	,208	18,500	,950
		Lower-bound	3,149	1,000	3,149	5,792	,025	,208	5,792	,633
	HQS	Sphericity Assumed	41,130	4	10,282	48,454	,000	,688	193,817	1,000
		Greenhouse-Geisser	41,130	3,213	12,801	48,454	,000	,688	155,686	1,000
		Huynh-Feldt	41,130	3,827	10,747	48,454	,000	,688	185,441	1,000
		Lower-bound	41,130	1,000	41,130	48,454	,000	,688	48,454	1,000
Error(interface)	PQ	Sphericity Assumed	11,961	88	,136					
		Greenhouse-Geisser	11,961	60,693	,197					
		Huynh-Feldt	11,961	70,263	,170					
		Lower-bound	11,961	22,000	,544					
	HQS	Sphericity Assumed	18,674	88	,212					
		Greenhouse-Geisser	18,674	70,687	,264					
		Huynh-Feldt	18,674	84,197	,222					
		Lower-bound	18,674	22,000	,849					

a. Computed using alpha = ,05

Pairwise Comparisons

Measure	(I) interface	(J) interface	Mean Difference (I-J)	Std. Error	Sig.[a]	95% Confidence Interval for Difference[a]	
						Lower Bound	Upper Bound
PQ	1	2	,161	,081	,601	-,093	,416
		3	,205	,071	,087	-,017	,427
		4	,335*	,106	,047	,003	,668
		5	,491*	,127	,008	,096	,886
	2	1	-,161	,081	,601	-,416	,093
		3	,043	,105	1,000	-,285	,372
		4	,174	,136	1,000	-,251	,599
		5	,329	,136	,242	-,095	,753
	3	1	-,205	,071	,087	-,427	,017
		2	-,043	,105	1,000	-,372	,285
		4	,130	,078	1,000	-,112	,373
		5	,286	,109	,152	-,053	,624
	4	1	-,335*	,106	,047	-,668	-,003
		2	-,174	,136	1,000	-,599	,251
		3	-,130	,078	1,000	-,373	,112
		5	,155	,115	1,000	-,202	,513
	5	1	-,491*	,127	,008	-,886	-,096
		2	-,329	,136	,242	-,753	,095
		3	-,286	,109	,152	-,624	,053
		4	-,155	,115	1,000	-,513	,202
HQS	1	2	-,174	,095	,796	-,469	,121
		3	-1,186*	,133	,000	-1,601	-,771
		4	-1,429*	,119	,000	-1,799	-1,058
		5	-1,261*	,133	,000	-1,676	-,846
	2	1	,174	,095	,796	-,121	,469
		3	-1,012*	,173	,000	-1,553	-,472
		4	-1,255*	,133	,000	-1,669	-,840
		5	-1,087*	,148	,000	-1,547	-,627
	3	1	1,186*	,133	,000	,771	1,601
		2	1,012*	,173	,000	,472	1,553
		4	-,242	,139	,946	-,675	,190
		5	-,075	,147	1,000	-,534	,385
	4	1	1,429*	,119	,000	1,058	1,799
		2	1,255*	,133	,000	,840	1,669
		3	,242	,139	,946	-,190	,675
		5	,168	,125	1,000	-,223	,559
	5	1	1,261*	,133	,000	,846	1,676
		2	1,087*	,148	,000	,627	1,547
		3	,075	,147	1,000	-,385	,534
		4	-,168	,125	1,000	-,559	,223

Based on estimated marginal means

a. Adjustment for multiple comparisons: Bonferroni.
*. The mean difference is significant at the ,05 level.

A.3.4.3 Preference

Ranks

	Mean Rank
PrefSelHHD	2,00
PrefSelSW	3,89
PrefSelHMD	2,78
PrefSelSWRef	3,09
PrefSelBodyRef	3,24

Test Statistics[a]

N	23
Chi-Square	17,577
df	4
Asymp. Sig.	,001

a. Friedman Test

The p-values in the following table are not Bonferroni corrected. Bonferroni corrected values are p-value*0.1

Test Statistics[c]

	PrefSelSW - PrefSelHHD	PrefSelHMD - PrefSelHHD	PrefSelSWRef - PrefSelHHD	PrefSelBody Ref - PrefSelHHD	PrefSelHMD - PrefSelSW	PrefSelSWRef - PrefSelSW	PrefSelBody Ref - PrefSelSW	PrefSelSWRef - PrefSelHMD	PrefSelBody Ref - PrefSelHMD	PrefSelBody Ref - PrefSelSWRef
Z	-4,145[a]	-1,476[a]	-2,291[a]	-2,408[a]	-2,178[b]	-1,513[b]	-1,393[b]	-,632[a]	-,925[a]	-,309[a]
Asymp. Sig. (2-tailed)	,000	,140	,022	,016	,029	,130	,163	,527	,355	,758

a. Based on negative ranks.
b. Based on positive ranks.
c. Wilcoxon Signed Ranks Test

Bibliography

[A+97] Ronald T Azuma et al. A survey of augmented reality. *Presence*, 6(4):355–385, 1997. 15

[AHY+15] Youngseok Ahn, Sungjae Hwang, HyunGook Yoon, Junghyeon Gim, and Jung-hee Ryu. Bandsense: Pressure-sensitive multi-touch interaction on a wristband. In *Proceedings of the 33rd Annual ACM Conference Extended Abstracts on Human Factors in Computing Systems*, pages 251–254. ACM, 2015. 17

[BBB+10] Sebastian Boring, Dominikus Baur, Andreas Butz, Sean Gustafson, and Patrick Baudisch. Touch projector: mobile interaction through video. In *Proceedings of the SIGCHI Conference on Human Factors in Computing Systems*, pages 2287–2296. ACM, 2010. 18

[BBDM98] Mark Billinghurst, Jerry Bowskill, Nick Dyer, and Jason Morphett. An evaluation of wearable information spaces. In *Virtual Reality Annual International Symposium, 1998. Proceedings., IEEE 1998*, pages 20–27. IEEE, 1998. 18

[BGL05] Mark Billinghurst, Raphael Grasset, and Julian Looser. Designing augmented reality interfaces. *ACM Siggraph Computer Graphics*, 39(1):17–22, 2005. 18

[BGS01] Patrick Baudisch, Nathaniel Good, and Paul Stewart. Focus plus context screens: combining display technology with visualization techniques. In *Proceedings of the 14th annual ACM symposium on User interface software and technology*, pages 31–40. ACM, 2001. 22, 27

[BIF05] Hrvoje Benko, Edward W Ishak, and Steven Feiner. Cross-dimensional gestural interaction techniques for hybrid immersive environments. In *Virtual Reality, 2005. Proceedings. VR 2005. IEEE*, pages 209–216. IEEE, 2005. 18

[BLB+03] Stephen Brewster, Joanna Lumsden, Marek Bell, Malcolm Hall, and Stuart Tasker. Multimodal'eyes-free'interaction techniques for wearable devices. In *Proceedings of the SIGCHI conference on Human factors in computing systems*, pages 473–480. ACM, 2003. 17

[BLB13] Rahul Budhiraja, Gun A Lee, and Mark Billinghurst. Using a hhd with a hmd for mobile ar interaction. In *Mixed and Augmented Reality (ISMAR), 2013 IEEE International Symposium on*, pages 1–6. IEEE, 2013. 18

[BS99] Mark Billinghurst and Thad Starner. Wearable devices: new ways to manage information. *Computer*, 32(1):57–64, 1999. 17, 18

[BSP+93] Eric A Bier, Maureen C Stone, Ken Pier, William Buxton, and Tony D DeRose. Toolglass and magic lenses: the see-through interface. In *SIGGRAPH*, pages 73–80. ACM, 1993. 24

[Cab10] Ricardo Cabello. Three.js. *URL: https://github.com/mrdoob/three.js*, 2010. 34

[CB06] Xiang Cao and Ravin Balakrishnan. Interacting with dynamically defined information spaces using a handheld projector and a pen. In *Proceedings of the 19th annual ACM symposium on User interface software and technology*, pages 225–234. ACM, 2006. 17

[CGWF14] Xiang'Anthony' Chen, Tovi Grossman, Daniel J Wigdor, and George Fitzmaurice. Duet: exploring joint interactions on a smart phone and a smart watch. In *Proceedings of the 32nd annual ACM conference on Human factors in computing systems*, pages 159–168. ACM, 2014. 18

[CMT+12] Xiang'Anthony' Chen, Nicolai Marquardt, Anthony Tang, Sebastian Boring, and Saul Greenberg. Extending a mobile device's interaction space through body-centric interaction. In *Proceedings of the 14th international conference on Human-computer interaction with mobile devices and services*, pages 151–160. ACM, 2012. 17, 28

[CQG+11] Andy Cockburn, Philip Quinn, Carl Gutwin, Gonzalo Ramos, and Julian Looser. Air pointing: Design and evaluation of spatial target acquisition with and without visual feedback. *International Journal of Human-Computer Studies*, 69(6):401–414, 2011. 17

[DCN13] William Delamare, Céline Coutrix, and Laurence Nigay. Designing disambiguation techniques for pointing in the physical world.

In *Proceedings of the 5th ACM SIGCHI symposium on Engineering interactive computing systems*, pages 197–206. ACM, 2013. 17, 25

[EFI14] Barrett M Ens, Rory Finnegan, and Pourang P Irani. The personal cockpit: a spatial interface for effective task switching on head-worn displays. In *Proceedings of the 32nd annual ACM conference on Human factors in computing systems*, pages 3171–3180. ACM, 2014. 17

[EHRI14] Barrett Ens, Juan David Hincapié-Ramos, and Pourang Irani. Ethereal planes: a design framework for 2d information space in 3d mixed reality environments. In *SUI 14*, pages 2–12. ACM, 2014. 20, 22

[Fit93] George W Fitzmaurice. Situated information spaces and spatially aware palmtop computers. *Communications of the ACM*, 36(7):39–49, 1993. 17

[FMHS93] Steven Feiner, Blair MacIntyre, Marcus Haupt, and Eliot Solomon. Windows on the world: 2d windows for 3d augmented reality. In *Proceedings of the 6th annual ACM symposium on User interface software and technology*, pages 145–155. ACM, 1993. 17

[GHQS15] Jens Grubert, Matthias Heinisch, Aaron John Quigley, and Dieter Schmalstieg. Multifi: multi-fidelity interaction with displays on and around the body. In *Proceedings of the SIGCHI conference on Human Factors in computing systems*. ACM Press-Association for Computing Machinery, 2015. 12

[GMB+11] Saul Greenberg, Nicolai Marquardt, Till Ballendat, Rob Diaz-Marino, and Miaosen Wang. Proxemic interactions: the new ubicomp? *interactions*, 18(1):42–50, 2011. 20

[GPG+14] Jens Grubert, Michel Pahud, Raphael Grasset, Dieter Schmalstieg, and Hartmut Seichter. The utility of magic lens interfaces on handheld devices for touristic map navigation. *Pervasive and Mobile Computing*, 2014. 40

[GSW+00] Yakup Genc, Frank Sauer, Fabian Wenzel, Mihran Tuceryan, and Nassir Navab. Optical see-through hmd calibration: A stereo method validated with a video see-through system. In *Augmented*

Reality, 2000.(ISAR 2000). Proceedings. IEEE and ACM International Symposium on, pages 165–174. IEEE, 2000. 35

[GTMS10] Jens Grubert, Johannes Tuemle, Ruediger Mecke, and Michael Schenk. Comparative user study of two see-through calibration methods. *VR*, 10:269–270, 2010. 16

[HBK03] Marc Hassenzahl, Michael Burmester, and Franz Koller. Attrakdiff: Ein fragebogen zur messung wahrgenommener hedonischer und pragmatischer qualität. In *Mensch & Computer 2003*, pages 187–196. Springer, 2003. 38, 57

[HRG+04] Ken Hinckley, Gonzalo Ramos, Francois Guimbretiere, Patrick Baudisch, and Marc Smith. Stitching: pen gestures that span multiple displays. In *Proceedings of the working conference on Advanced visual interfaces*, pages 23–31. ACM, 2004. 18

[HS88] Sandra G Hart and Lowell E Staveland. Development of nasa-tlx (task load index): Results of empirical and theoretical research. *Advances in psychology*, 52:139–183, 1988. 38, 57

[HZ04] R. I. Hartley and A. Zisserman. *Multiple View Geometry in Computer Vision*. Cambridge University Press, ISBN: 0521540518, 2004. 16, 35

[Joh14] Kyle Mills Johnson. Literature review: An investigation into the usefulness of the smart watch interface for university students and the types of data they would require. 2014. 17

[LB03] Joanna Lumsden and Stephen Brewster. A paradigm shift: alternative interaction techniques for use with mobile & wearable devices. In *Proceedings of the 2003 conference of the Centre for Advanced Studies on Collaborative research*, pages 197–210. IBM Press, 2003. 17

[LDT09] Frank Chun Yat Li, David Dearman, and Khai N Truong. Virtual shelves: interactions with orientation aware devices. In *Proceedings of the 22nd annual ACM symposium on User interface software and technology*, pages 125–128. ACM, 2009. 17, 28

[Lew91] James R Lewis. Psychometric evaluation of an after-scenario questionnaire for computer usability studies: the asq. *ACM SIGCHI Bulletin*, 23(1):78–81, 1991. 38, 57

[LF05] Vincent Lepetit and Pascal Fua. Monocular model-based 3d tracking of rigid objects: A survey. *Foundations and trends in computer graphics and vision*, 1(CVLAB-ARTICLE-2005-002):1–89, 2005. 15

[LXC+14] Gierad Laput, Robert Xiao, Xiang'Anthony' Chen, Scott E Hudson, and Chris Harrison. Skin buttons: cheap, small, low-powered and clickable fixed-icon laser projectors. In *Proceedings of the 27th annual ACM symposium on User interface software and technology*, pages 389–394. ACM, 2014. 17

[MK94] Paul Milgram and Fumio Kishino. A taxonomy of mixed reality visual displays. *IEICE TRANSACTIONS on Information and Systems*, 77(12):1321–1329, 1994. 15

[MTUK95] Paul Milgram, Haruo Takemura, Akira Utsumi, and Fumio Kishino. Augmented reality: A class of displays on the reality-virtuality continuum. In *Photonics for industrial applications*, pages 282–292. International Society for Optics and Photonics, 1995. 15

[OFH08] Alex Olwal, Steven Feiner, and Susanna Heyman. Rubbing and tapping for precise and rapid selection on touch-screen displays. In *Proceedings of the SIGCHI Conference on Human Factors in Computing Systems*, pages 295–304. ACM, 2008. 17

[PF93] Ken Perlin and David Fox. Pad: an alternative approach to the computer interface. In *SIGGRAPH 93*, pages 57–64. ACM, 1993. 24

[PHI+13] Michel Pahud, Ken Hinckley, Shamsi Iqbal, Abigail Sellen, and Bill Buxton. Toward compound navigation tasks on mobiles via spatial manipulation. In *Proceedings of the 15th international conference on Human-computer interaction with mobile devices and services*, pages 113–122. ACM, 2013. 17

[RB09] Julie Rico and Stephen Brewster. Gestures all around us: User differences in social acceptability perceptions of gesture based interfaces. In *MobileHCI 09*, pages 64:1–64:2, New York, NY, USA, 2009. ACM. 22

[Rei93] Bruce A Reichlen. Sparcchair: A one hundred million pixel display. In *Virtual Reality Annual International Symposium, 1993., 1993 IEEE*, pages 300–307. IEEE, 1993. 17

[Rei01] Tumasch Reichenbacher. Adaptive concepts for a mobile cartography. *Journal of Geographical Sciences*, 11(1):43–53, 2001. 40

[RHF95] Jannick P Rolland, Richard L Holloway, and Henry Fuchs. Comparison of optical and video see-through, head-mounted displays. In *Photonics for Industrial Applications*, pages 293–307. International Society for Optics and Photonics, 1995. 15

[RNQ12] Umar Rashid, Miguel A Nacenta, and Aaron Quigley. The cost of display switching: a comparison of mobile, large display and hybrid ui configurations. In *Proceedings of the International Working Conference on Advanced Visual Interfaces*, pages 99–106. ACM, 2012. 40

[SSP+14] Jie Song, Gábor Sörös, Fabrizio Pece, Sean Ryan Fanello, Shahram Izadi, Cem Keskin, and Otmar Hilliges. In-air gestures around unmodified mobile devices. In *Proceedings of the 27th annual ACM symposium on User interface software and technology*, pages 319–329. ACM, 2014. 17

[TIHS+01] Russell M Taylor II, Thomas C Hudson, Adam Seeger, Hans Weber, Jeffrey Juliano, and Aron T Helser. Vrpn: a device-independent, network-transparent vr peripheral system. In *Proceedings of the ACM symposium on Virtual reality software and technology*, pages 55–61. ACM, 2001. 33

[TN00] Mihran Tuceryan and Nassir Navab. Single point active alignment method (spaam) for optical see-through hmd calibration for ar. In *Augmented Reality, 2000.(ISAR 2000). Proceedings. IEEE and ACM International Symposium on*, pages 149–158. IEEE, 2000. 16, 35

[VB07] Daniel Vogel and Patrick Baudisch. Shift: a technique for operating pen-based interfaces using touch. In *Proceedings of the SIGCHI conference on Human factors in computing systems*, pages 657–666. ACM, 2007. 17

[WF02] Greg Welch and Eric Foxlin. Motion tracking survey. *IEEE Computer graphics and Applications*, pages 24–38, 2002. 15

[WNG+13] Julie Wagner, Mathieu Nancel, Sean G Gustafson, Stéphane Huot, and Wendy E Mackay. Body-centric design space for multi-surface interaction. In *Proceedings of the SIGCHI Conference on*

Human Factors in Computing Systems, pages 1299–1308. ACM, 2013. 17, 18

[YW14] Jishuo Yang and Daniel Wigdor. Panelrama: enabling easy specification of cross-device web applications. In *Proceedings of the 32nd annual ACM conference on Human factors in computing systems*, pages 2783–2792. ACM, 2014. 18

[ZSRB14] Jian Zhao, R William Soukoreff, Xiangshi Ren, and Ravin Balakrishnan. A model of scrolling on touch-sensitive displays. *International Journal of Human-Computer Studies*, 72(12):805–821, 2014. 43